# **QUARTERLY REPORT**

July 1, 2025 - September 30, 2025

# Kentucky Tobacco Research & Development Center





Martin-Gatton College of Agriculture, Food and Environment

### **MEMORANDUM**

DATE: October 31, 2025

TO: Kentucky Tobacco Research Board Members

Legislative Research Commission

FROM: Dr. Ling Yuan

Managing Director, KTRDC

SUBJECT: Kentucky Tobacco Research & Development Center

Quarterly Report for July 1, 2025 - September 30, 2025

Enclosed is a copy of the Kentucky Tobacco Research & Development Center's Quarterly Report for July 1, 2025 – September 30, 2025.

If you have any questions, please feel welcome to contact me at (859) 257-5798 or email lyuan3@uky.edu.

Enc.

# **TABLE OF CONTENTS**

		Page
Executive S	ummary	1
Report #1	"Exploring the Microbial Diversity and Composition of Three Cigar Product Categories".	9
	Sanjay Joshi, Kent Pham, Luke Moe, Ruth McNees	
Report #2	"A Cotyledon-based Virus-Induced Gene Silencing (Cotyledon-VIGS) approach to study specialized metabolism in medicinal plants".	19
	Yongliang Liu, Ruiqing Lyu, Joshua J. Singleton, Barunava Patra, Sitakanta Pattanaik, and Ling Yuan.	
Financial Re	eport	31

#### **EXECUTIVE SUMMARY**

### Introduction

The legislation (KRS 248.510 - 248.580) which provides funds in support of the research programs at the Kentucky Tobacco Research and Development Center (KTRDC) requires that a quarterly research report be submitted to the Kentucky Tobacco Research Board (KTRB) and the Legislative Research Commission.

The overall reporting plan is:

January 1 - March 31: Selected topics April 1 - June 30: Selected topics July 1 - September 30: Selected topics

October 1 - December 31: Annual comprehensive report

As required by KRS 248.570, a financial report covering expenditures for the relevant proportion of the July 1, 2025 – June 30, 2026 fiscal year is included in this report.

The news and research publications provided in this quarterly report are a representative selection of the Center's output. For a full description of all KTRDC research and activities please refer to the KTRDC Annual Report.

# Quarterly News

- KTRDC is collaborating with the UK Cannabis Center to produce cannabis for clinical behavioral studies. The cannabis plants will be grown in a specially adapted secure growth room. Low delta-9tetrahydrocannabinol (THC) hemp plants have been successfully grown in the growth room to test the facility. Currently, KTRDC is waiting on further instructions from the DEA.
- This quarter is always a busy time for the field group.
  - Activities at the university farm during this period were mainly sampling, topping, harvesting and selecting/bagging.
    - July was very hot and dry. With the late start to the season, no topping of agronomic trials was done in July. Topping and suckering were done in a contact seed yield trial.
    - August's activities were mainly topping and suckeride application.
       Topping of the agronomic trial was done on August 11. Selection

- and bagging were also done in August, and seed harvest of the seed yield trial began.
- September's activities were harvesting and seed collection, with harvesting completed on September 11. Selection/bagging continued, and by the end of September, the only plants left in the field were those for seed collection, and the seed yield trial. The harvested tobacco is now curing.
- There were originally work on two farms: the green burley farm test in Bourbon County and the CORESTA black shank variety trial in Clark County.
  - The on-farm green burley was abandoned after excessively hot dry weather at transplanting caused loss of most of the transplants.
  - Disease counts were done on the black shank trial in Clark County every two weeks until September 4. Soil samples were also collected from within the rows every four weeks.
- The September board meeting was held in KTRDC conference room and by Zoom.
  - Lesley Oliver, Associate Director, Kentucky Agricultural Experiment Station, talked about the USDA Civil Rights compliance requirement and asked board members to complete a demographic data form. As part of our civil rights compliance process, we are required to collect self-identified demographic information for members of all advisory boards. This is voluntarily and confidential and only used for reporting to the USDA for compliance with federal laws.
  - Elections were held for the Chairman and Vice Chairman of the KTRB.
     Mr. Todd Clark was elected to remain Chairman of the board and Mr.
     Al Pedigo was elected to remain Vice Chair of the KTRB.
  - Dr. Yuan, to clear up any confusion with income and the declining tax revenue, discussed the KTRDC finances and explained how KTRDC is two units, with the other being CTRP (Center for Tobacco Reference Products). He presented information regarding income vs expenses and talked about other funding available that is not part of the cigarette tax funds. CTRP funds were created from FDA grants and sale of reference products. Unfortunately, the FDA grants have ended and future grants are uncertain at this time.
  - Dr. Barun Patra gave a presentation entitled "Research Projects to Benefit Kentucky Tobacco Farmers". The presentation by Dr. Barunava Patra focused on current research initiatives at KTRDC to

address the major challenges facing Kentucky tobacco farmers. It was noted that extreme weather events such as drought and flooding, along with persistent disease pressures, pose serious threats to crop yield and quality. Research is focused on developing stress-tolerant plants, particularly through improvements in root system architecture that enhance water and nutrient uptake, as well as on building disease resistance using genetic tools.

The presentation also highlighted work on antifungal proteins such as NaD1, which shows strong activity against key fungal pathogens affecting tobacco. Strategies include directed evolution to improve antifungal performance and transgenic approaches to provide durable resistance, reducing the need for chemical fungicides. These projects aim to strengthen crop resilience, improve leaf quality, and secure the long-term sustainability of tobacco farming in Kentucky.

- Abstracts accepted and presentations for the two main tobacco conferences.
  - Abstracts for the CORESTA conference were submitted in late May. One paper, three reports and one poster from KTRDC were presented for the CORESTA congress in October. The Agro-Phyto Conference was held in Surabaya, Indonesia and attended by Anne Fisher, Colin Fisher, and Sitakanta Pattanaik. The Science-Techno Conference was held in Annecy, France and attended by Huihua Ji.
  - Abstracts for the TSRC conference were submitted in late May. One paper and two posters from KTRDC were presented for the conference in September, held in Knoxville, TN and attended by Ruth McNees, Huihua Ji, Ying, Wu, Anne Fisher, and Colin Fisher. Anne Fisher was awarded the 2025 TSRC Lifetime Achievement Award.
- The Center for Tobacco Reference Products (CTRP) proficiency testing (PT) program currently covers the certified reference cigarette, 1R6F, and the certified reference smokeless tobacco products, 1S4, 1S5, 3S1 and 3S3. CTRP is currently working with A2LA to add the newly produced certified reference cigars, 1RLC, 1RFC, and 1RSC, to the proficiency testing program. CTRP received an extension to the accreditation for proficiency testing to 2029.
  - The current PT rounds are:

- CIG-2025A The parameters for this round of testing include the smoking parameters Nicotine-Free Dry Particulate Matter (NFDPM/Tar), Nicotine, Carbon Monoxide, Water, Hydrogen Cyanide (HCN), Oxides of Nitrogen (NOx), Total Particulate Matter (TPM), and Puff Count using the 1R6F reference cigarette and the 2R5F low-deliverable reference cigarette as proficiency test material smoked in both Non-Intense and the Intense smoking regimes. This round of testing opened in January 2025. Due to multiple international laboratories experiencing issues with importing the test material, the deadline for uploading data was extended from April 2025 to May 2025. The interim report was released for participant review in June 2025 and the final report was released in July 2025.
- CIG-2025B The parameters for this round of testing include the smoking parameters NNK (4-(methylnitrosamino)-1-(3-pyridyl)-1butanone), NNN (N-nitrosonornicotine), NAT (N-nitrosoanatabine), NAB (N-nitrosoanabasine), Total Particulate Matter (TPM), and Puff Count using the 1R6F reference cigarette as proficiency test material smoked in both Non-Intense and the Intense smoking regimes. This test also includes the determination of physical properties of the test material namely: cigarette resistance to draw (pressure drop open), cigarette resistance to draw (pressure drop closed), filter pressure drop (fully encapsulated), total ventilation, filter ventilation, tobacco weight, cigarette weight, air permeability, firmness, circumference, cigarette length, filter plug length, and tipping paper length. This round of testing opened in March 2025. Due to multiple international laboratories experiencing issues with importing the test material, the deadline for uploading data was extended from June 2025 to August 2025. The interim report was released for participant review in August 2025 and the final report was released in September 2025.
- CIG-2025C The parameters for this round of testing include cigarette filler analysis for Oven Volatiles (Moisture), pH, Total Nicotine, NNN (N-nitrosonornicotine), NNK (4-(methylnitrosamino)-1-(3-pyridyl)-1-butanone), NAT (N-nitrosoanatabine), NAB (N-nitrosoanabasine), Arsenic (As), Cadmium (Cd), and Ammonia (NH3) using the 1R6F reference cigarette as proficiency test material. This round of testing opened in May 2025. The data portal for participants to upload data is scheduled to close in September 2025, but extended to October 2025. The interim report was

- expected to be released in October 2025 and the final report in November 2025.
- SMK-2025D The parameters for this round of testing include analysis of 1S5 (Snus) and 3S1 (Loose Leaf Chewing Tobacco) for Total Nicotine, Free Nicotine, NNK (4-(methylnitrosamino)-1-(3-NNN (N-nitrosonornicotine), pyridyl)-1-butanone), nitrosoanatabine), NAB (N-nitrosoanabasine), Acetaldehyde. Crotonaldehyde. Formaldehyde, Benzo[α]pyrene, Cadmium. Arsenic, pH, and Moisture. This round of testing opened in August 2025. The deadline for uploading data is set for January 2026. The interim report is scheduled to be released for participant review in January 2026 and the final report is scheduled to be released in February 2026.

I would like to thank Ms. Anne Fisher, Ms. Cindy Stidham, and Dr. Ruth McNees for their help with preparing this report.

The KTRDC Quarterly Reports include copies and brief summaries of work published by KTRDC scientists and scientists partly funded by KTRDC.

Report #1 "Exploring the Microbial Diversity and Composition of Three Cigar Product Categories".

Sanjay Joshi, Kent Pham, Luke Moe, Ruth McNees

This research provides an overview of the total bacterial population within various cigar products sampled from three different cigar product categories. High throughput sequencing of the V4 hypervariable region of the 16 s rRNA gene was employed to identify bacteria within a complex population. The composition of the bacterial population was compared within and across product types to identify unique and shared bacteria within the various product categories.

Cigars and cigarillos are emerging as popular tobacco alternatives to cigarettes. However, these products may be equally harmful to human health than cigarettes and are associated with similar adverse health effects. We used 16S rRNA gene amplicon sequencing to extensively characterize the microbial diversity and investigate differences in microbial composition across 23 different products representing three different cigar product categories: filtered cigar, cigarillo, and large cigar. High throughput sequencing of the V4 hypervariable region of the 16 s rRNA gene revealed 2124 Operational Taxonomic Units (OTUs). Our findings showed that the three categories of cigars differed significantly in observed richness and Shannon diversity, with filtered cigars exhibiting lower diversity compared to large cigars and cigarillos. We also found a shared and unique microbiota among different product types. Firmicutes was the most abundant phylum in all product categories, followed by Actinobacteria. Among the 16 genera all product types were *Bacillus*, Staphylococcus, across Pseudomonas, and Pantoea. Nine genera were exclusively shared by large cigars and cigarillos and an additional thirteen genera were exclusive to filtered cigars. Analysis of individual cigar products showed consistent microbial composition across replicates for most large cigars and cigarillos while filtered cigars showed more inter-product variability. These findings provide important insights into the microbial diversity of the different cigar product types.

Report #2 "A Cotyledon-based Virus-Induced Gene Silencing (Cotyledon-VIGS) approach to study specialized metabolism in medicinal plants".

Yongliang Liu, Ruiqing Lyu, Joshua J. Singleton, Barunava Patra, Sitakanta Pattanaik, and Ling Yuan.

The cotyledon-based VIGS method is faster, more efficient, and easily accessible to additional treatments than the traditional VIGS method. Cotyledon-VIGS overcomes several issues facing the previously established VIGS methods and can be used for other non-model plant species. Although a protocol optimized for one species might work for other species, the parameters still need to be fine-tuned for each plant species to achieve optimal results. Each plant species is different with respect to germination time, size, and morphology of the cotyledon, as well as the sensitivity to Agrobacterium infection. In our study, the parameters that worked well for C. roseus did not yield the best results for G. inflata and A. annua. Therefore, certain conditions, such as age of the seedling, density (OD<sub>600</sub>) of Agrobacterium-suspension, and infiltration time, should be optimized for each plant species to achieve optimal results.

Virus-induced gene silencing (VIGS) is widely used in plant functional genomics. However, the efficiency of VIGS in young plantlets varies across plant species. Additionally, VIGS is not optimized for many plant species, especially medicinal plants that produce valuable specialized metabolites. We evaluated the efficacy of five-day-old, etiolated seedlings of Catharanthus roseus (periwinkle) for VIGS. The seedlings were vacuuminfiltrated with Agrobacterium tumefaciens GV3101 cells carrying the tobacco rattle virus (TRV) vectors. The protoporphyrin IX magnesium chelatase subunit H (ChlH) gene, a key gene in chlorophyll biosynthesis, was used as the target for VIGS, and we observed yellow cotyledons 6 days after infiltration. As expected, the expression of CrChIH and the chlorophyll contents of the cotyledons were significantly decreased after VIGS. To validate the cotyledon based-VIGS method, we silenced the genes encoding several transcriptional regulators of the terpenoid indole alkaloid (TIA) biosynthesis in C. roseus, including two activators (CrGATA1 and CrMYC2) and two repressors (CrGBF1 and CrGBF2). Silencing CrGATA1 led to downregulation of the vindoline pathway genes (T3O, T3R, and DAT) and decreased vindoline contents in cotyledons. Silencing CrMYC2, followed by elicitation with methyl jasmonate (MeJA), resulted in the downregulation of

ORCA2 and ORCA3. We also co-infiltrated C. roseus seedlings with TRV vectors that silence both CrGBF1 and CrGBF2 and overexpress CrMYC2, aiming to simultaneous silencing two repressors while overexpressing an activator. The simultaneous manipulation of repressors and activator resulted in significant upregulation of the TIA pathway genes. To demonstrate the broad application of the cotyledon-based VIGS method, we optimized the method for two other valuable medicinal plants, Glycyrrhiza inflata (licorice) and Artemisia annua (sweet wormwood). When TRV vectors carrying the fragments of the ChIH genes were infiltrated into the seedlings of these plants, we observed yellow cotyledons with decreased chlorophyll contents. The widely applicable cotyledon-based VIGS method is faster, more efficient, and easily accessible to additional treatments than the traditional VIGS method. It can be combined with transient gene overexpression to achieve simultaneous up- and down-regulation of desired genes in non-model plants. This method provides a powerful tool for functional genomics of medicinal plants, facilitating the discovery and production of valuable therapeutic compounds.

#### RESEARCH



# **Exploring the Microbial Diversity and Composition of Three Cigar Product Categories**

Sanjay Joshi<sup>1</sup> · Kent Pham<sup>2</sup> · Luke Moe<sup>2</sup> · Ruth McNees<sup>1</sup>

Received: 16 May 2024 / Accepted: 9 August 2024 © The Author(s) 2024

#### Abstract

Cigars and cigarillos are emerging as popular tobacco alternatives to cigarettes. However, these products may be equally harmful to human health than cigarettes and are associated with similar adverse health effects. We used 16S rRNA gene amplicon sequencing to extensively characterize the microbial diversity and investigate differences in microbial composition across 23 different products representing three different cigar product categories: filtered cigar, cigarillo, and large cigar. High throughput sequencing of the V4 hypervariable region of the 16 s rRNA gene revealed 2124 Operational Taxonomic Units (OTUs). Our findings showed that the three categories of cigars differed significantly in observed richness and Shannon diversity, with filtered cigars exhibiting lower diversity compared to large cigars and cigarillos. We also found a shared and unique microbiota among different product types. *Firmicutes* was the most abundant phylum in all product categories, followed by *Actinobacteria*. Among the 16 genera shared across all product types were *Bacillus*, *Staphylococcus*, *Pseudomonas*, and *Pantoea*. Nine genera were exclusively shared by large cigars and cigarillos and an additional thirteen genera were exclusive to filtered cigars. Analysis of individual cigar products showed consistent microbial composition across replicates for most large cigars and cigarillos while filtered cigars showed more inter-product variability. These findings provide important insights into the microbial diversity of the different cigar product types.

Keywords Cigar · Cigarillo · Filtered cigar · 16S rRNA gene amplicon sequencing · Microbiome

#### Introduction

Cigars in all product categories are emerging as popular tobacco products due to multiple factors that include lower cost as a result of the lower taxation rate when compared to cigarettes and the addition of flavors to cigar products [1, 2]. In recent years, cigars have become the most reported combustible tobacco product used by youth [3, 4]. A study conducted in the United States in 2020 of almost one million middle and high school students that self-reported having smoked cigars in the past 30 days, showed that the largest proportion of students reported using cigarillos (44.1%), followed by traditional cigars (33.1%), and filtered cigars

(22.6%) [5, 6]. In this study, we focus on three different types of cigars, namely large (traditional) cigars, filtered cigars, and cigarillos. Large cigars come in a range of sizes and are made up of tobacco wrapped in leaf tobacco or homogenized tobacco leaf (HTL) material. Cigarillos are similar to large cigars but may be thinner and longer than a normal cigarette, while filtered cigars resemble cigarettes but are wrapped with HTL [7]. Cigar products are manufactured using specific varieties of tobacco which typically undergo a fermentation process that impacts the microbial population [8]. Additionally, the commercially available products used in this study use homogenized tobacco leaves for wrapper and binders, where applicable, as not all products contain both wrapper and binder. The products were expected to have differences as a result of the blend and ratio of the variety of cigar tobacco used to make the filler, the region of tobacco growth impacts the quality, and manufacturing processes. Contrary to popular belief, cigars are not less toxic than cigarettes but are associated with the same adverse health effects, including addiction to nicotine, oral lesions, oral cancer, lung cancer, cardiovascular disease, and

Published online: 20 August 2024



Ruth McNees ruth.mcnees@uky.edu

Kentucky Tobacco Research and Development Center (KTRDC), University of Kentucky, Lexington, KY 40546, USA

Department of Plant and Soil Sciences, University of Kentucky, Lexington, KY 40546, USA

107 Page 2 of 10 S. Joshi et al.

chronic obstructive pulmonary disease [9–12]. Some studies have suggested that cigar products may be more harmful to human health than cigarettes [13–15]. Tobacco-specific nitrosamines (TSNAs) are a class of harmful compounds known to be carcinogenic and the formation of TSNAs has been shown to correlate with microbial metabolic activities [16, 17]. By studying microbial communities in cigars, organisms and pathways relating to the formation and possible reduction of TSNAs in tobacco products may be unveiled [18].

In this study, we use 16S rRNA gene amplicon to characterize the bacterial communities of cigar products in multiple product categories. 16S rRNA gene amplicon study is useful when examining multiple taxonomic domains simultaneously, especially when some of the microbes are not visually different and cannot be cultured in media [19]. Similar culture-independent methods have been used to investigate the microbial diversity of tobacco products, which revealed increased diversity compared to traditional culture-based approaches [18, 20]. We utilized the MiSeq platform to sequence the V4 region of samples representative of multiple cigar product categories which then allowed us to compare the similarities and differences between product types and analyze the associated microbial communities. The objective of the study is to extensively characterize microbial populations in cigar products that will fill a research gap and provide data to assess the potential health impact of cigars, providing important insights for the development of more effective tobacco control policies and public health interventions.

#### **Materials and Methods**

#### **Sample Collection and DNA Extraction**

A total of 23 different cigar products were obtained from online vendors and commercial distributors, including four research cigars (1C1, 1C2, 1C3, and 1C4) from the Center for Tobacco Reference Products (CTRP) at Kentucky Tobacco Research and Development Center (University of Kentucky, USA). The commercially available products were selected based on market share and sales within the United States to provide a comprehensive overview of the microbial compositions. The products were categorized into three groups: large standard cigars, filtered cigars, and cigarillos, consisting of five, six, and eight brands, respectively (Table 1). Cigars were randomly selected from the commercial packaging. Filtered cigars were selected from three packs within a carton, and 3 filtered cigars were randomly selected from various locations within each pack. Cigarillos were selected from three foil packs within an upright containing 15 foil packs, the industrial standard for packaging

Table 1 Tabulation of the different cigar products used with their name and category

Large cigars	Filtered cigars	Cigarillos
1C1	1C2	1C3
1C4	Phillies	Phillies Black
William Penn	Captain Black	Phillies Sweet
Garcia y Vega	King Edward	White Owl black
White Owl	Talon	White Owl silver
Swisher Sweets	Cheyenne	Black & Mild
<b>Dutch Masters</b>	Djarum	Pom Pom sweet
		<b>Dutch Masters</b>
		Swisher Sweets

of cigarillos, and only one of the two cigarillos was used for analysis. The large cigars were randomly selected from a box of cigars containing up to 50 individually wrapped cigars. For all products tested, all tobacco material was homogenized prior to DNA extraction. DNA extraction was performed on freshly opened packages of all products using the ZymoBIOMICS<sup>TM</sup> DNA miniprep D4300 kit (Zymo Research, Irvine, CA, USA) and following the manufacturer's recommended protocol. The extracted DNA was quantified using QUBIT 4.0. To minimize variability, we performed three technical replicates for each biological replicate, and three biological replicates were taken. The technical replicates were combined prior to sequencing to ensure that the data presented in the figures represent the averaged result of the technical replicates, thereby reducing technical variability. To ensure sterility, each product was opened under sterile conditions, homogenized in sterile saline solution (0.85%) using a bag mixer, filtered, and processed according to the kit instructions.

### Sequencing and Analysis of 16S rRNA Gene Sequences

We shipped the DNA samples from cigar products to The University of Michigan, Microbial Systems Molecular Biology Laboratory core sequencing facility (http://microbe.med.umich.edu/services/microbial-community-analysis) for PCR amplification and sequencing of the V4 region of the 16S rRNA gene on the Illumina MiSeq platform (dual-barcoded, paired-end reads, 2×250 flow cell) according to Kozich, et al. [21]. Sequence data from MiSeq sequencing was processed using MOTHUR software (v1.48.5) following the MiSeq SOP (https://www.mothur.org/wiki/MiSeq\_SOP, accessed January 2023) [22]. We followed the analysis methodology previously published by Law et al., 2020, using the SILVA reference alignment of the MOTHUR-formatted version of the RDP training set (SSU Silva 138 v.18) for classification [23, 24]. The cigar data set was subsampled and



normalized to 3436 sequences per sample, which resulted in 2124 OTUs (operational taxonomic units) after classification at the 0.03 cutoff level. Raw sequence reads for all samples in this study were uploaded to the NCBI Bio Project database under accession number PRJNA1073920.

Statistical analysis was performed using the built-in functions in MOTHUR [22]. We compared bacterial community structure using the analysis of similarities function (ANO-SIM) [25]. Observed Richness and Shannon's diversity were calculated in MOTHUR and imported into the R program to compare alpha diversity measures and abundance using the Kruskal–Wallis rank sum test, with any significant results further tested by Dunn's test [26]. The package ggplot2 was used to plot the data generated from MOTHUR [27]. The Venn diagram was made using VENNY 2.1 [28].

#### Results

#### **Sequencing Dataset and Diversity**

In this study, we extracted DNA from 69 different samples of cigar and cigarillo products, resulting in a total of 2,308,008 raw sequencing reads. After filtering out PCR and sequencing errors, 2,147,392 reads remained, leaving us with an error rate of 0.95%. We used Good's coverage estimator to confirm that all samples had sufficient sampling depth, with values greater than 98.84%. We then calculated alpha diversity, which is based on the number of species within a sample, and measures for richness and Shannon diversity. We then compared them across cigar types using the nonparametric Kruskal-Wallis rank sum test. Our results indicate that the three categories of cigars (large, filtered, cigarillos) differ significantly in observed richness and Shannon diversity. Specifically, filtered cigars showed lower observed richness and Shannon diversity compared to large cigars and cigarillos, with large cigars having the highest measure of alpha diversity (Fig. 1). The Kruskal-Wallis rank sum test revealed a chi-squared value of 10.02 with a p-value of 0.01 for Shannon diversity. Using the Dunn test with Holm correction, we found a significant reduction in Shannon diversity in filtered cigars compared to both large cigars and cigarillos. Additionally, we observed that the microbial populations of filtered cigars were statistically different from those of cigarillos (p = 0.0388) and large cigars (p = 0.0026), while the microbial populations of cigarillos and large cigars were not statistically different.

Furthermore, we employed Principal Coordinate Analysis (PCoA) to assess the dissimilarity of various cigar samples based on Bray-Curtis distances plotted as the results in Fig. 2. Subsequently, we subjected the data to the ANOSIM test, which yielded an R statistic value of 0.193, and the significance level was set at 0.001. These

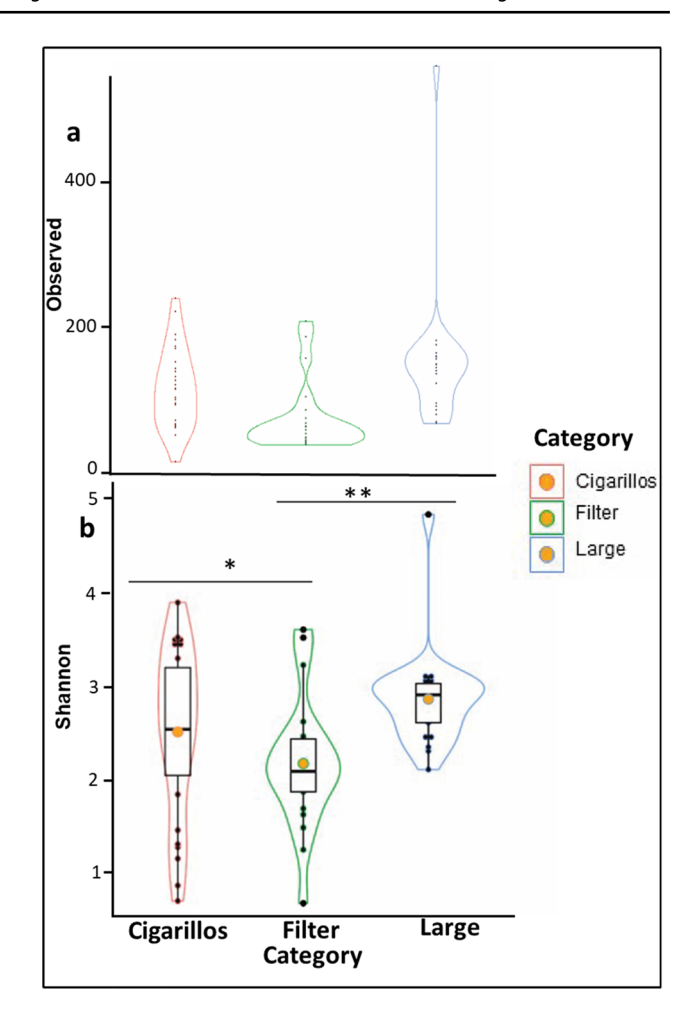


**Fig. 1** Alpha diversity (**a**) Observed richness (**b**) Shannon diversity by product category (Lines connecting box plots indicate significant difference using the Dunn test. (\*\* P < 0.01; \*P < 0.05). Filtered cigars showed lower observed richness and Shannon diversity compared to large cigars and cigarillos, with large cigars having the highest measure of alpha diversity

findings indicate the presence of significant beta diversity, which compares the diversity across samples, among the three cigar categories. Beta diversity analysis is crucial for comparing the diversity between different environments or groups, even when raw materials, formulations, and processes differ. It highlights differences in the presence or absence and abundance of microbial species among cigar types. This approach allows us to understand the distinct microbial communities associated with each cigar product category. When comparing filtered cigars with cigarillos, the computed R-value was 0.29 at a significance level of 0.01, indicating a substantial dissimilarity between the two groups. Similarly, the comparison between filtered cigars and large cigars also exhibited a significant level of dissimilarity. However, in contrast, the comparison between large cigars and cigarillos did not reach a level of statistical significance (Table 2).



107 Page 4 of 10 S. Joshi et al.

Fig. 2 Principal component analysis (PCoA) of Bray–Curtis distances between cigar samples of different product categories. The ellipse is drawn at a 90% confidence level. PCoA analysis indicated significant differences in beta diversity measures between the three cigar categories

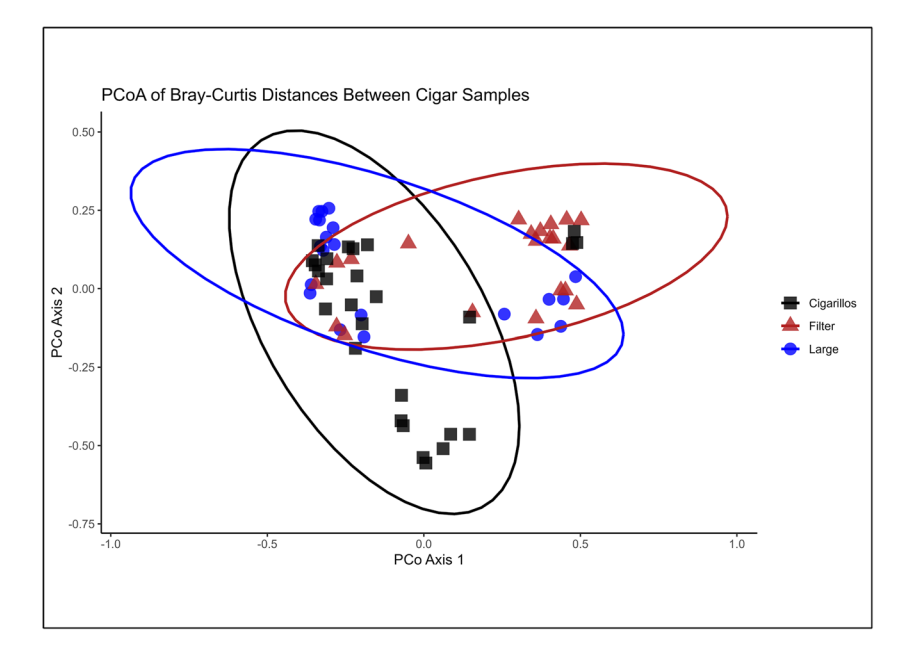


**Table 2** Analysis of Similarities (ANOSIM) test with distance and category of product. Pairwise comparison using Mothur for each product type. Experiment-wise error rate: 0.05, pairwise error rate (Bonferroni): 0.0167. Microbial populations of filtered cigars are statistically different from those of cigarillos and large cigars

Group Comparison	R-value	P-value
Cigarillos-Filter-Large	0.19	< 0.001*
Cigarillos-Filter	0.291	0.001*
Cigarillos-Large	0.044	0.087
Filter-Large	0.257	< 0.001*

#### **Core and Shared Microbiomes Across Products**

In our study, we clustered the overall sequences into 2124 Operational Taxonomic Units (OTUs) with 97% identity across all 69 cigar samples. The top five bacterial phyla identified across all cigar types were Firmicutes, Actinobacteria, Proteobacteria, Acidobacteria, and Bacteroidetes. The most abundant phyla in all product categories were Firmicutes, followed by Actinobacteria. Filtered cigars exhibited a slightly higher abundance of Firmicutes (91.12%) compared to large cigars (70.29%) and cigarillos (81.55%), while also showing a decrease in Actinobacteria (2.09%) compared to large cigars (16.42%) and cigarillos (8.05%) (Fig. 3a). When we compared the top 30 genera for the three cigar categories, 16 genera (33.3%) were shared among all product types, while nine genera were specifically shared only by large cigars and cigarillos. Apart from the core microbiome, there was no genus similarity between filtered cigars and large cigars (Fig. 3b). However, there were 13 exclusive genera only for filtered cigars. The list of shared and unique genera for each cigar type is provided in Table 3.

### **Microbial Populations Within each Category**

#### **Total Genus Population Within Filtered Cigars**

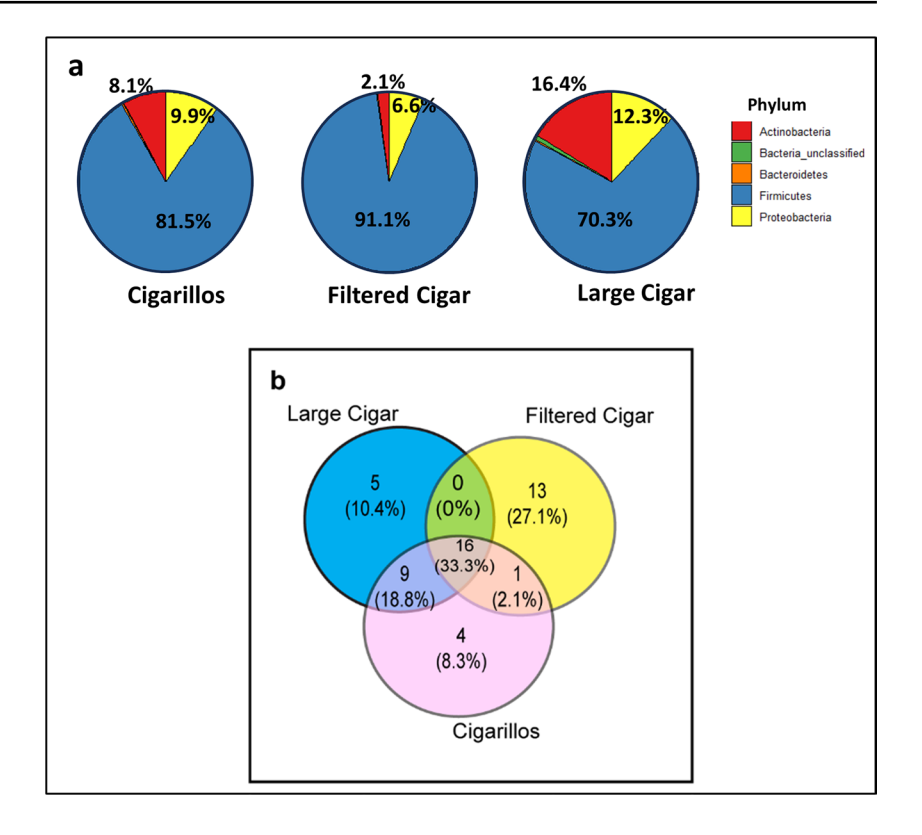
We analyzed seven different filtered cigars including one research filtered cigar (1C2). The top twenty genera of each product type were assessed based on the most numerous OTUs. The filtered cigars 1C2 and Phillies had uniform microbiome composition for each replicate (Fig. 4). Other products including Captain Black, Djarum, Talon, and Cheyenne have similar microbiomes for two of the three replicates. Djarum, the only filtered cigar product tested that included cloves with tobacco, had a higher percentage of *Bacillus* and *Staphylococcus* populations compared to other filtered cigars, whereas 1C2 and Talon had higher *Tissierella* genus. Of the seven products in the filtered cigar category, only the King Edward samples were significantly different for each replicate tested, making it difficult to determine the microbial population of this product.

#### **Total Genus Population Within Cigarillos**

In the case of cigarillos, we tested nine products. Cigarillo samples had a more consistent and uniform microbiome composition between the replicates. The research cigarillo (1C3), Black and Mild, White Owl Black, White Owl Silver, and Swisher Sweets have uniform microbiomes for each replicate (Fig. 5). For Black and mild, *Pseudomonas* represented more than 40% of the microbial population, and *Pantoea* represented 12% of the population which was the highest compared to other cigarillo types. White Owl Black and White Owl Silver had the highest percentage of *Staphylococcus* compared to the other products tested. Swisher Sweets and PomPom had



Fig. 3 Core and shared microbiome in different categories in (a) Phylum level showing in each category in percentage (b) Genus level similarity and specific to each category in Venn diagram



a higher percentage of *Terribacillus* compared to other products, and they had similar microbiomes for two of the three replicates. *Bacillus* was the most common genus present in most samples. Two out of three replicates of Phillies Sweet showed higher levels of *Lentibacillus*. Dutch Masters and Phillies Black samples were different for each replicate.

#### **Total Genus Population Within Large Cigars**

A total of seven products in the large cigar category were taken including two research cigar products (1C1 and 1C4). All products have a uniform microbiome for each replicate, except White Owl which had a consistent microbiome for two of the three replicates. All large cigar samples show a higher percentage (8.20–39.46%) of *Staphylococcus* genus except William Penn and Garcia y Vega (0.16–2.09%) (Fig. 6). Additionally, these products showed an increased percentage of *Planococcaceae unclassified* (17.62–36.70%) and *Paenibacillus* (0.72–4.3%) which was observed at low levels for the other products tested (0.01–0.08%, with one replicate on the 1C4 having 2.3%).

#### **Discussion**

The use of 16S rRNA gene amplicon sequencing allowed for a comprehensive characterization of the microbial diversity of cigar and cigarillo products, revealing differences between product types and providing information on various microbial populations. This study explores the microbial diversity of large cigars, filtered cigars, and cigarillos, to provide insight into the composition of the microbial communities that are unique and shared in these products. Our study revealed a significant difference in microbial diversity among the three categories of cigars (large, filtered, cigarillos) based on alpha diversity measures for richness and Shannon diversity. Specifically, filtered cigars exhibited lower diversity compared to both large cigars and cigarillos. PCoA analysis with the ANOSIM test indicated significant differences in beta diversity measures between the three cigar categories, with the microbial populations of filtered cigars being statistically different from those of cigarillos and large cigars. Furthermore, when comparing the top 30 genera for the three cigar categories, the core microbiome analysis revealed that 16 genera were shared among all three categories of cigars, while nine genera were shared only by large cigars and cigarillos. These shared genera such as Oceanobacillus, Corynebacterium, Staphylococcus, Bacillus, and Pseudomonas are commonly found as the most predominant genera in tobacco products [29, 30]. The first three genera are shown to have a direct effect on the fermentation process [31–33]. Additionally, our study identified 13 exclusive genera only for filtered cigars, such as Tissierella, and Clostridium\_XlVa. In contrast, there was no genus similarity between filtered cigars and large cigars (Table 3).



107 Page 6 of 10 S. Joshi et al.

Table 3 List of genera shared and unique to specific cigar category types

#### 1 genus in "Filtered Cigar" and "Cigarillos" 16 common genera in all products 9 common genera in "Large Cigar" and 'Cigarillos' Bacillus Yaniella Paenibacillaceae 1 unclassified Acinetobacter Lentibacillus Brachybacterium Aerococcus Bacillaceae\_2\_unclassified Gracilibacillus Bacillales\_unclassified Atopostipes Brevibacterium Tetragenococcus Corvnebacterium Geomicrobium Enterobacteriaceae\_unclassified Aurantimonas Oceanobacillus Rhodobacteraceae\_unclassified Paenibacillus Pantoea Planococcaceae\_unclassified Pseudomonas Sphingomonas Staphylococcus Terribacillus 13 genera exclusively in "Filtered Cigar" 5 genera exclusively in "Large Cigar" only 4 genera exclusively in "Cigarillos" only only Tissierella Ralstonia Sedimentibacter Clostridium\_XlVa Bacteria\_unclassified Weissella Planococcaceae\_incertae\_sedis Desemzia Thermoactinomyces Sporomusa Stenotrophomonas Actinomycetales\_unclassified Staphylococcaceae\_unclassified Enterococcus Lachnospiraceae\_unclassified Veillonellaceae unclassified Firmicutes\_unclassified Garciella Bacilli\_unclassified Clostridiales\_unclassified Clostridium\_sensu\_stricto Dendrosporobacter

The presence of certain genera in all cigar types suggests the existence of a core microbiome in these products. However, there was no significant difference between the microbial populations of cigarillos and large cigars. The differences observed in the microbial composition of filtered cigars compared to large cigars and cigarillos could be due to the type of cigar tobacco (filler leaf, wrapper leaf), the region the tobacco was grown, the fermentation method during curing, or the manufacturing process. The most abundant phyla across all product categories were Firmicutes, followed by Actinobacteria, which agrees with similar studies to the one presented here [33-35]. Interestingly, filtered cigars had a slightly higher abundance of Firmicutes compared to large cigars and cigarillos, while also showing a decrease in Actinobacteria. A recent study showed that filtered cigar products have a unique bacterial signature and certain genera such as *Enterobacteriaceae*,

Pantoea, Pseudomonas, and Staphylococcus were more abundant in the cigar tobacco used to produce the filtered cigar [1]. Microbial diversity studies conducted on cigarettes and various tobacco products, including smokeless forms, have uncovered a similar microbial population as found in the current study of cigar products [36]. Research on Burley and Flue-cured tobacco leaves has found Bacillus and Pseudomonas to be the predominant genera, while Proteobacteria is the dominant phylum, comprising over 90% of the operational taxonomic units (OTUs) in burley tobacco leaves [36, 37]. A recent study where sequencing was performed on the samples cultured from the mainstream smoke of unfiltered cigarettes showed Bacillus, Terribacillus, Paenibacillus, and Desulfotomaculum as their predominant genera [38]. Furthermore, bacterial community profiling in smokeless tobacco products revealed Firmicutes, Proteobacteria, Actinobacteria and Bacteroidetes as dominant



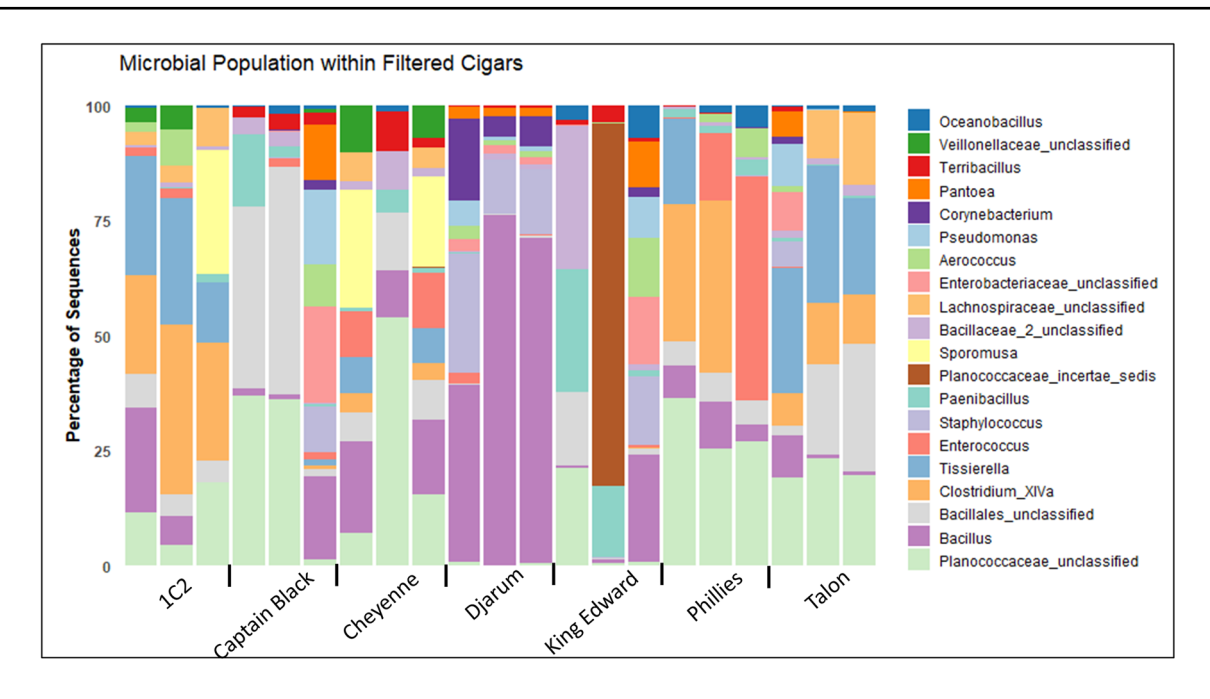


Fig. 4 Stacked bar chart showing the percentage of the dominant top 20 genera within the microbial population of each filtered cigar sample

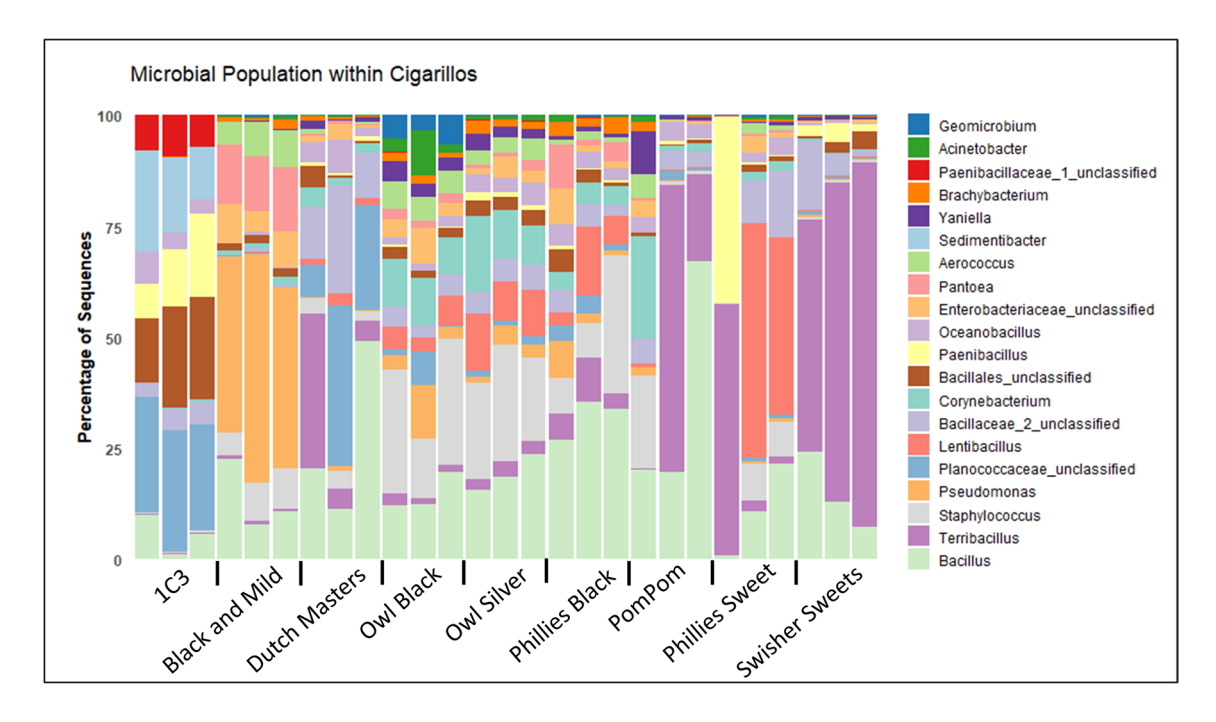


Fig. 5 Stacked bar chart showing the dominant top 20 genera of each cigarillos

phyla and *Acinetobacter*, *Bacillus*, *Prevotella*, *Acetobacter*, *Lactobacillus* were enriched bacterial genera. Additionally, microbial diversity and composition were determined to be variable across multiple smokeless tobacco product types and brands [18, 39–41].

We evaluated for inter-product variability within the microbiome composition of seven different filtered cigars,

nine cigarillos, and seven large cigars. The filtered cigars 1C2 and Phillies had a uniform microbiome composition for each replicate, while other products showed some variability. Djarum had a higher percentage of *Bacillus* and *Staphylococcus* population, while 1C2 and Talon had a higher *Tissierella* genus. Cigarillo samples had a more consistent and uniform microbiome composition between



107 Page 8 of 10 S. Joshi et al.

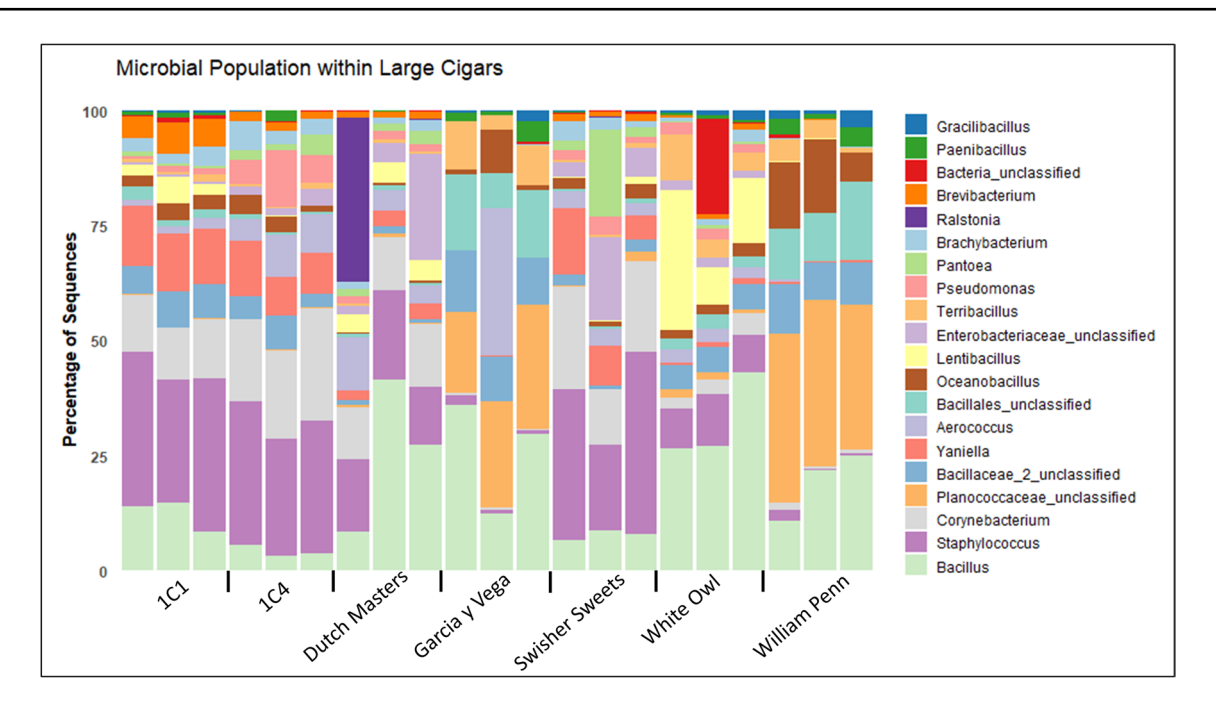


Fig. 6 Stacked bar chart showing the dominant top 20 genera of each large cigar

the replicates, and Bacillus was the most common genus present in all samples. Compared to the other cigar categories, large cigars showed the highest percentage of Staphylococcus genus, except for William Penn and Gracia y Vega, which showed an increased percentage of Planococcaceae unclassified and Paenibacillus. There could be several factors causing the variation among the products, natural differences in the microbial populations between individual cigars as a result of the blend of tobacco used in manufacturing. The impact on the microbial population as a result of the manufacturer was not investigated for this study, as many manufacturers have production facilities in multiple locations, oftentimes in different countries. A study, conducted by Di Giacomo et al. (2007) on the microbial community in Italian Toscano cigar tobacco during fermentation, observed changes in the relative abundances of specific microbial groups over time [20]. They found that Bacillus species, including B. licheniformis and B. subtillis, could reduce NO<sub>3</sub> without producing N<sub>2</sub> gas, while Corynebacterium ammonia genes accumulated nitrite during subsequent stages of tobacco maturation. During the curing process of tobacco, changes in microbial communities were observed as nutrients were depleted, pH changed, moisture evaporated, and temperature increased. It also demonstrated a gradual decrease in tobacco pH, which was attributed to the metabolic byproducts of acidproducing species [20]. Various discrepancies in abundance and composition are not unexpected considering that brands are manufactured under different industrial conditions with proprietary tobacco blends. Another study showed that filtered cigar microbiome composition was dynamic and influenced by environmental factors such as temperature, humidity, and storage time [42].

Overall, our study provides new insights into the microbial diversity and composition of different categories of cigars, highlighting the impact of various cigar types and sizes on microbial populations. These findings hold significant implications for the regulation of tobacco products and the comprehension of potential health impacts arising from smoking diverse types of cigars. Prior research has demonstrated the abundance of human pathogens in tobacco products, particularly in cigarettes and smokeless tobacco, which could result in the development of chronic or infectious respiratory disease, as well as cancer [43–46]. Similarly, it is crucially important for further studies to elucidate the functional roles of these microorganisms in cigar products. In future studies, it may be possible to link pathogenicity to the microbial population as species with the genera *Bacillus*, Staphylococcus, and Pseudomonas have been identified as human pathogens. The use of MiSeq technology could be limited due to amplification bias, sequencing errors, and taxonomic resolutions. Utilizing advanced sequencing technologies and conducting experiments to identify metabolically active bacteria [34] could be one of the several approaches to dissecting the impact of microbes on human health. A recent study highlighted how viable bacteria could survive cigarette combustion and then be transferred to the upper respiratory system via mainstream smoke [38]. Additionally, future studies could focus on variation within microbiomes based on various production locations for specific manufacturers.



**Author Contribution** SJ and RM contributed to the design and implementation of the research. SJ and KP contributed to the analysis of the sequences. SJ, KP, LM, and RM contributed to the writing and reviewing of the manuscript.

**Funding** This work was supported by the Food and Drug Administration (grant UC2FD006890). The views expressed in written materials or publications and by speakers and moderators do not necessarily reflect the official policies of the Department of Health and Human Services nor does any mention of trade names, commercial practices, or organization imply endorsement by the United States Government.

**Data Availability** Sequences can be found in the NCBI SRA database under the Bio project accession number PRJNA1073920.

#### **Declarations**

Competing Interests The authors declare no competing interests.

Open Access This article is licensed under a Creative Commons Attribution-NonCommercial-NoDerivatives 4.0 International License, which permits any non-commercial use, sharing, distribution and reproduction in any medium or format, as long as you give appropriate credit to the original author(s) and the source, provide a link to the Creative Commons licence, and indicate if you modified the licensed material. You do not have permission under this licence to share adapted material derived from this article or parts of it. The images or other third party material in this article are included in the article's Creative Commons licence, unless indicated otherwise in a credit line to the material. If material is not included in the article's Creative Commons licence and your intended use is not permitted by statutory regulation or exceeds the permitted use, you will need to obtain permission directly from the copyright holder. To view a copy of this licence, visit http://creativecommons.org/licenses/by-nc-nd/4.0/.

#### References

- Smyth EM, Chattopadhyay S, Babik K, Reid M, Chopyk J, Malayil L, Kulkarni P, Hittle LE, Clark PI, Sapkota AR (2019) The bacterial communities of little cigars and cigarillos are dynamic over time and varying storage conditions. Front Microbiol 10:2371
- Chattopadhyay S, Smyth EM, Kulkarni P, Babik KR, Reid M, Hittle LE, Clark PI, Mongodin EF, Sapkota AR (2019) Little cigars and cigarillos harbor diverse bacterial communities that differ between the tobacco and the wrapper. PLoS One 14:e0211705. https://doi.org/10.1371/journal.pone.0211705
- Wang TW, Gentzke AS, Creamer MR, Cullen KA, Holder-Hayes E, Sawdey MD, Anic GM, Portnoy DB, Hu S, Homa DM (2019) Tobacco product use and associated factors among middle and high school students—United States, 2019. MMWR Surveill Summ 68:1
- Phan L, McNeel TS, Chen-Sankey J, Niederdeppe J, Tan ASL, Choi K (2022) US trends in age of cigar smoking initiation by race/ethnicity and education. Am J Prev Med 63:624–629. https:// doi.org/10.1016/j.amepre.2022.04.004
- Gentzke AS, Wang TW, Cornelius M, Park-Lee E, Ren C, Sawdey MD, Cullen KA, Loretan C, Jamal A, Homa DM (2022) Tobacco product use and associated factors among middle and high school students—National Youth Tobacco Survey, United States, 2021. MMWR Surveill Summ 71:1

- Parms TA, Head SK, Sawdey MD, Rostron BL, Cullen KA (2022) Characteristics of past 30-day cigar smoking, U.S. Adolescents, 2020. Am J Prev Med 62:e39–e44. https://doi.org/10.1016/j.amepre.2021.06.011
- Milam AJ, Bone L, Furr-Holden D, Coylewright M, Dachille K, Owings K, Clay E, Holmes W, Lambropoulos S, Stillman F (2012) Mobilizing for policy: using community-based participatory research to impose minimum packaging requirements on small cigars. Prog Community Health Partnersh 6:205–212. https://doi.org/10.1353/cpr.2012.0027
- Zhang Y, Xu Q, Yang M, Yang Y, Fu J, Miao C, Wang G, Hu L, Hu Z (2023) Analysis of differences in tobacco leaf microbial communities after redrying in Chinese provinces and from abroad. AMB Express 13:80. https://doi.org/10.1186/s13568-023-01580-5
- Paulin LM, Halenar MJ, Edwards KC, Lauten K, Stanton CA, Taylor K, Hatsukami D, Hyland A, MacKenzie T, Mahoney MC, Niaura R, Trinidad D, Blanco C, Compton WM, Gardner LD, Kimmel HL, Lauterstein D, Marshall D, Sargent JD (2022) Association of tobacco product use with chronic obstructive pulmonary disease (COPD) prevalence and incidence in Waves 1 through 5 (2013–2019) of the Population Assessment of Tobacco and Health (PATH) Study. Resp Res 23:273. https://doi.org/10.1186/ s12931-022-02197-1
- Baker F, Ainsworth SR, Dye JT, Crammer C, Thun MJ, Hoffmann D, Repace JL, Henningfield JE, Slade J, Pinney J, Shanks T, Burns DM, Connolly GN, Shopland DR (2000) Health risks associated with cigar smoking. JAMA 284:735–740. https://doi.org/10.1001/ jama.284.6.735
- Chen-Sankey JC, Mead-Morse EL, Le D, Rose SW, Quisenberry AJ, Delnevo CD, Choi K (2021) Cigar-smoking patterns by race/ ethnicity and cigar type: a nationally representative survey among US adults. Am J Prev Med 60:87–94
- Chang CM, Corey CG, Rostron BL, Apelberg BJ (2015) Systematic review of cigar smoking and all cause and smoking related mortality. BMC Public Health 15:1–20
- Richardson A, Xiao HJ, Val DM (2012) Primary and dual users of cigars and cigarettes: profiles, tobacco use patterns, and relevance to policy. Nicotine Tob Res 14:927–932. https://doi.org/10.1093/ ntr/ntr306
- Symm B, Morgan MV, Blackshear Y, Tinsley S (2005) Cigar smoking: an ignored public health threat. J Prim Prev 26:363–375. https://doi.org/10.1007/s10935-005-5389-z
- Ross JC, Suerken CK, Reboussin BA, Denlinger-Apte RL, Spangler JG, Sutfin EL (2022) Cigar harm beliefs and associations with cigar use among young adults. Subst Use Misuse 57:1478–1485. https://doi.org/10.1080/10826084.2022.2092149
- Humans IWGotEoCRt (2007) Smokeless tobacco and some tobacco-specific N-nitrosamines. IARC Monogr Eval Carcinog Risks Hum 89:1–592
- Law AD, Fisher C, Jack A, Moe LA (2016) Tobacco, microbes, and carcinogens: correlation between tobacco cure conditions, tobacco-specific nitrosamine content, and cured leaf microbial community. Microb Ecol 72:120–129. https://doi.org/10.1007/ s00248-016-0754-4
- Rivera AJ, Tyx RE (2021) Microbiology of the American Smokeless Tobacco. Appl Microbiol Biotechnol 105:4843–4853. https://doi.org/10.1007/s00253-021-11382-z
- Tessler M, Cunningham SW, Ingala MR, Warring SD, Brugler MR (2023) An environmental DNA primer for microbial and restoration ecology. Microb Ecol. https://doi.org/10.1007/s00248-022-02168-5
- Di Giacomo M, Paolino M, Silvestro D, Vigliotta G, Imperi F, Visca P, Alifano P, Parente D (2007) Microbial community structure and dynamics of dark fire-cured tobacco fermentation. Appl Environ Microbiol 73:825–837. https://doi.org/10.1128/Aem. 02378-06



107 Page 10 of 10 S. Joshi et al.

- Kozich JJ, Westcott SL, Baxter NT, Highlander SK, Schloss PD (2013) Development of a dual-index sequencing strategy and curation pipeline for analyzing amplicon sequence data on the MiSeq Illumina sequencing platform. Appl Environ Microbiol 79:5112–5120
- Schloss PD, Westcott SL, Ryabin T, Hall JR, Hartmann M, Hollister EB, Lesniewski RA, Oakley BB, Parks DH, Robinson CJ (2009) Introducing mothur: open-source, platform-independent, community-supported software for describing and comparing microbial communities. Appl Environ Microbiol 75:7537–7541
- Cole JR, Wang Q, Fish JA, Chai B, McGarrell DM, Sun Y, Brown CT, Porras-Alfaro A, Kuske CR, Tiedje JM (2014) Ribosomal Database Project: data and tools for high throughput rRNA analysis. Nucleic Acids Res 42:D633-642. https://doi.org/10.1093/nar/ gkt1244
- Law AD, McNees CR, Moe LA (2020) The microbiology of hemp retting in a controlled environment: steering the hemp microbiome towards more consistent fiber production. Agronomy 10:492
- Clarke KR (1993) Non-parametric multivariate analyses of changes in community structure. Aust J Ecol 18:117–143
- Dinno A (2015) Nonparametric pairwise multiple comparisons in independent groups using Dunn's test. Stand Genomic Sci 15:292–300
- Wickham H, Chang W, Henry L, Pendersen T, Takahashi K, Wilke C, Woo K, Yutani H, Dunnington D (2016) ggplot2: elegant graphics for data analysis.[Google Scholar]
- Oliveros JC (2007) VENNY. An interactive tool for comparing lists with Venn Diagrams. http://bioinfogp.cnb.csic.es/tools/venny/index.html. Accessed July 2023
- Chattopadhyay S, Malayil L, Mongodin EF, Sapkota AR (2021) A roadmap from unknowns to knowns: advancing our understanding of the microbiomes of commercially available tobacco products. Appl Microbiol Biotechnol 105:2633–2645
- Kumar RS, Mishra N, Kumar A (2022) Characterization of tobacco microbiome by metagenomics approach. Methods Mol Biol 2413:229–244. https://doi.org/10.1007/978-1-0716-1896-7\_ 22
- Gao R, Sun-Waterhouse D, Xiang H, Cui C, Waterhouse GI (2022)
   The effect of the Corynebacterium glutamicum on the shortening of fermentation time, physicochemical and sensory properties of soy sauce. Int J Food Sci Technol 57:4316

  –4327
- 32. Jia Y, Niu C-T, Xu X, Zheng F-Y, Liu C-F, Wang J-J, Lu Z-M, Xu Z-H, Li Q (2021) Metabolic potential of microbial community and distribution mechanism of Staphylococcus species during broad bean paste fermentation. Food Res Int 148:110533
- Liu T, Guo S, Wu C, Zhang R, Zhong Q, Shi H, Zhou R, Qin Y, Jin Y (2022) Phyllosphere microbial community of cigar tobacco and its corresponding metabolites. Front Microbiol 13:1025881. https://doi.org/10.3389/fmicb.2022.1025881
- Chattopadhyay S, Ramachandran P, Malayil L, Mongodin EF, Sapkota AR (2023) Conventional tobacco products harbor unique and heterogenous microbiomes. Environ Res 220:115205. https:// doi.org/10.1016/j.envres.2022.115205

- 35. Huang Y, Wang H-C, Cai L-T, Li W, Pan D, Xiang L, Su X, Li Z, Adil MF, Shamsi IH (2021) Phyllospheric microbial composition and diversity of the tobacco leaves infected by Didymella segeticola. Front Microbiol 12:699699
- Pauly JL, Paszkiewicz G (2011) Cigarette smoke, bacteria, mold, microbial toxins, and chronic lung inflammation. J Oncol 2011:819129. https://doi.org/10.1155/2011/819129
- Huang J, Yang J, Duan Y, Gu W, Gong X, Zhe W, Su C, Zhang K-Q (2010) Bacterial diversities on unaged and aging flue-cured tobacco leaves estimated by 16S rRNA sequence analysis. Appl Microbiol Biotechnol 88:553–562. https://doi.org/10.1007/s00253-010-2763-4
- Malayil L, Chattopadhyay S, Mongodin EF, Sapkota AR (2022) Bacterial communities of hookah tobacco products are diverse and differ across brands and flavors. Appl Microbiol Biotechnol 106:5785–5795. https://doi.org/10.1007/s00253-022-12079-7
- Sajid M, Srivastava S, Kumar A, Kumar A, Singh H, Bharadwaj M (2021) Bacteriome of moist smokeless tobacco products consumed in India with emphasis on the predictive functional potential. Front Microbiol 12:784841
- Smyth EM, Kulkarni P, Claye E, Stanfill S, Tyx R, Maddox C, Mongodin EF, Sapkota AR (2017) Smokeless tobacco products harbor diverse bacterial microbiota that differ across products and brands. Appl Microbiol Biotechnol 101:5391–5403. https://doi. org/10.1007/s00253-017-8282-9
- 41. Vishwakarma A, Verma D (2020) 8 Exploring the microbiome of smokeless tobacco. In: Chowdhary P, Raj A, Verma D, Akhter Y (eds.) Microorganisms for sustainable environment and health. Elsevier, pp 167-178. https://doi.org/10.1016/B978-0-12-819001-2.00008-5
- 42. Chopyk J, Chattopadhyay S, Kulkarni P, Smyth EM, Hittle LE, Paulson JN, Pop M, Buehler SS, Clark PI, Mongodin EF (2017) Temporal variations in cigarette tobacco bacterial community composition and tobacco-specific nitrosamine content are influenced by brand and storage conditions. Front Microbiol 8:358
- Simba H, Menya D, Mmbaga BT, Dzamalala C, Finch P, Mlombe Y, Mremi A, Narh CT, Schuz J, McCormack V (2023) The contribution of smoking and smokeless tobacco to oesophageal squamous cell carcinoma risk in the African oesophageal cancer corridor: results from the ESCCAPE multicentre case-control studies. Int J Cancer. https://doi.org/10.1002/ijc.34458
- Sawant S, Dugad J, Parikh D, Srinivasan S, Singh H (2023) Oral microbial signatures of tobacco chewers and oral cancer patients in India. Pathogens 12. https://doi.org/10.3390/pathogens120100 78
- Vishwakarma A, Srivastava A, Mishra S, Verma D (2022) Taxonomic and functional profiling of Indian smokeless tobacco bacteriome uncovers several bacterial-derived risks to human health.
   World J Microbiol Biotechnol 39:20. https://doi.org/10.1007/s11274-022-03461-8
- Sapkota AR, Berger S, Vogel TM (2010) Human pathogens abundant in the bacterial metagenome of cigarettes. Environ Health Perspect 118:351–356. https://doi.org/10.1289/ehp.0901201



#### METHODOLOGY Open Access

# Check for updates

# A Cotyledon-based Virus-Induced Gene Silencing (Cotyledon-VIGS) approach to study specialized metabolism in medicinal plants

Yongliang Liu<sup>1</sup>, Ruiging Lyu<sup>1</sup>, Joshua J. Singleton<sup>1</sup>, Barunava Patra<sup>1</sup>, Sitakanta Pattanaik<sup>1\*</sup> and Ling Yuan<sup>1\*</sup>

#### **Abstract**

**Background** Virus-induced gene silencing (VIGS) is widely used in plant functional genomics. However, the efficiency of VIGS in young plantlets varies across plant species. Additionally, VIGS is not optimized for many plant species, especially medicinal plants that produce valuable specialized metabolites.

Results We evaluated the efficacy of five-day-old, etiolated seedlings of Catharanthus roseus (periwinkle) for VIGS. The seedlings were vacuum-infiltrated with Agrobacterium tumefaciens GV3101 cells carrying the tobacco rattle virus (TRV) vectors. The protoporphyrin IX magnesium chelatase subunit H (ChIH) gene, a key gene in chlorophyll biosynthesis, was used as the target for VIGS, and we observed yellow cotyledons 6 days after infiltration. As expected, the expression of CrChIH and the chlorophyll contents of the cotyledons were significantly decreased after VIGS. To validate the cotyledon based-VIGS method, we silenced the genes encoding several transcriptional regulators of the terpenoid indole alkaloid (TIA) biosynthesis in C. roseus, including two activators (CrGATA1 and CrMYC2) and two repressors (CrGBF1 and CrGBF2). Silencing CrGATA1 led to downregulation of the vindoline pathway genes (T3O, T3R, and DAT) and decreased vindoline contents in cotyledons. Silencing CrMYC2, followed by elicitation with methyl jasmonate (MeJA), resulted in the downregulation of ORCA2 and ORCA3. We also co-infiltrated C. roseus seedlings with TRV vectors that silence both CrGBF1 and CrGBF2 and overexpress CrMYC2, aiming to simultaneous silencing two repressors while overexpressing an activator. The simultaneous manipulation of repressors and activator resulted in significant upregulation of the TIA pathway genes. To demonstrate the broad application of the cotyledon-based VIGS method, we optimized the method for two other valuable medicinal plants, Glycyrrhiza inflata (licorice) and Artemisia annua (sweet wormwood). When TRV vectors carrying the fragments of the ChIH genes were infiltrated into the seedlings of these plants, we observed yellow cotyledons with decreased chlorophyll contents.

**Conclusions** The widely applicable cotyledon-based VIGS method is faster, more efficient, and easily accessible to additional treatments than the traditional VIGS method. It can be combined with transient gene overexpression to achieve simultaneous up- and down-regulation of desired genes in non-model plants. This method provides

\*Correspondence: Sitakanta Pattanaik spatt2@uky.edu Ling Yuan lyuan3@uky.edu

Full list of author information is available at the end of the article



© The Author(s) 2024. **Open Access** This article is licensed under a Creative Commons Attribution 4.0 International License, which permits use, sharing, adaptation, distribution and reproduction in any medium or format, as long as you give appropriate credit to the original author(s) and the source, provide a link to the Creative Commons licence, and indicate if changes were made. The images or other third party material in this article are included in the article's Creative Commons licence, unless indicated otherwise in a credit line to the material. If material is not included in the article's Creative Commons licence and your intended use is not permitted by statutory regulation or exceeds the permitted use, you will need to obtain permission directly from the copyright holder. To view a copy of this licence, visit http://creativecommons.org/licenses/by/4.0/. The Creative Commons Public Domain Dedication waiver (http://creativecommons.org/publicdomain/zero/1.0/) applies to the data made available in this article, unless otherwise stated in a credit line to the data.

Liu et al. Plant Methods (2024) 20:26 Page 2 of 12

a powerful tool for functional genomics of medicinal plants, facilitating the discovery and production of valuable therapeutic compounds.

**Keywords** Cotyledon-VIGS, Catharanthus roseus, Glycyrrhiza inflata, Artemisia annua

#### **Background**

Virus-induced gene silencing (VIGS) has emerged as an invaluable tool for post-transcriptional gene silencing in plants [1-3]. Compared to conventional genetic transformation methods, VIGS offers several advantages, including rapid implementation, efficiency, low cost, and independence of tissue culture and plant regeneration processes. VIGS is thus particularly useful for many nonmodel and recalcitrant plants [1, 2, 4]. Various RNA and DNA viruses have been employed in VIGS, and among them, tobacco rattle virus (TRV) is widely used due to its broad host range, efficient silencing outcomes, and mild symptoms on plants [3, 5-7]. TRV-based VIGS has been successfully applied in a wide range of plant species, including model plants such as Arabidopsis thaliana [8], Nicotiana benthamiana [6] and tomato (Solanum lycopersicum) [9], crops such as wheat (Triticum aestivum) and maize (Zea mays) [10], and medicinal plants such as Catharanthus roseus (Madagascar periwinkle) [11-16] and Withania somnifera (winter cherry) [17]. Moreover, TRV-based VIGS have been applied to different plant organs, including roots [18, 19], leaves [9], flowers [20], fruits [21], and seeds [22], making it a versatile tool for functional genomic research. Despite the many advantages of TRV-based VIGS, its broader application is limited by several factors, including variations in inoculation methods, as well as low and inconsistent efficiency in various plant species [23].

Agroinfiltration methods, through syringe or vacuum infiltration, are commonly used to transiently overexpress or knockdown a gene-of-interest. In syringe infiltration, a needle-free syringe carrying Agrobacterium suspension is placed on abaxial surface of leaf lamina and the suspension is slowly forced into leaves. Initially, the syringe infiltration method has been used to inoculate Agrobacterium carrying TRV vectors into the leaves of N. benthamiana [6]. However, this method was found unsuitable for some of the other plant species, leading to the development of diverse inoculation methods such as spray infiltration [9], vacuum infiltration [24], pinch wounding [11], Agrodrench [19], and sprout vacuum infiltration (SVI) [25]. In vacuum infiltration, the pressure differences between the surface and the inside of the leaf causes the penetration of Agrobacterium into the leaf's intercellular space. Plant tissues immersed in Agrobacterium suspension is placed in a vacuum chamber. The pressure in the chamber is lowered for a short duration to release the air in the intercellular spaces through the stomata. The plant tissue is subjected to re-pressurization during which the suspension is drawn into the leaf through the stomata [26, 27]. For some plant species, determining the suitable inoculation method requires testing several different methods, which is time intensive. For example, four inoculation methods have been tested for C. roseus, and only the pinch wounding method is proven successful [11]. The SVI method has been optimized in four Solanaceous crops, including tomato, eggplant (Solanum melongena), pepper (Capsicum annuum), and N. benthamiana, and the method is faster than other inoculation methods, showing silencing phenotype in the first pair of true leaves [25]. However, the movement of the virus to the newly developed leaves, the efficiency and time vary in different plants. For instance, the efficiency of optimized SVI for two Lycium barbarum and L. ruthenicum (Goji) species only reaches approximately 30% [28]. Therefore, the development of a widely applicable and highly efficient method is necessary to advance VIGS technology.

C. roseus is a highly valued medicinal plant that accumulates almost 200 terpenoid indole alkaloids (TIAs), including the important anti-cancer drugs vinblastine and vincristine [29]. While the biosynthesis of TIAs in C. roseus has been extensively studied [30-32], efforts are still ongoing to better understand the regulatory mechanisms [33]. Methyl jasmonate (MeJA) is the major elicitor of TIA biosynthesis, and several transcription factors (TFs), such as CrMYC2 [34, 35], BISs [36-38], ORCAs [39-43], RMT1 [15] and CrGBFs [35, 44], have been characterized for their roles in the regulation of TIA biosynthesis in response to MeJA. The vindoline biosynthesis, which is not regulated by MeJA, is controlled by the GATA-type zinc-finger TF CrGATA1 [13]. To date, stable transformation to consistently generate transgenic C. roseus plants has been difficult. VIGS has been widely relied on by many laboratories in characterizing genes encoding biosynthetic enzymes, transporters, and regulators involved in TIA biosynthesis [13–15, 31, 45]. Because the complex, dimerized TIAs are synthesized in C. roseus leaves, transformation of hairy roots, although useful in genetic characterization, does not allow the investigation of TIA pathway genes that are predominantly expressed in the leaves. Like *C. roseus*, the generation of stable transgenic plants are difficult and time consuming for many other medicinal plants, such as Glycyrrhiza inflata [46] which produce the bioactive agent licochalcones. An efficient VIGS technique certainly benefits the studies of the biosynthesis and regulation of the specialized metabolites in these plants.

Liu et al. Plant Methods (2024) 20:26 Page 3 of 12

Here we describe the development of a cotyledonbased VIGS (cotyledon-VIGS) method for C. roseus, which is significantly faster and more efficient than the previously described pinch wounding method. We also successfully extended cotyledon-VIGS to medicinal plants G. inflata and Artemisia annua, indicating the broad applicability of the technique. Silencing CrGATA1 or CrMYC2 in C. roseus resulted in expected downregulation of their respective target genes and reduction in accumulation of TIAs. Additionally, we were able to silence two repressor CrGBFs and overexpress the activator CrMYC2 simultaneously by combining cotyledon-VIGS with a transient gene overexpression method. Our findings demonstrated that cotyledon-VIGS is a versatile tool for analysis of gene functions in recalcitrant medicinal and crop plants. A protocol optimized for one plant species might work for other species; however, the parameters should still be optimized for each plant species to achieve the best results.

#### Results

#### Five-day-old *C. roseus* seedlings are ideal for cotyledon-VIGS

The C. roseus seeds were germinated in the dark (Fig. 1af). The radicles were emerged from the seed coats on the second day (Fig. 1c), while the cotyledons fully emerged on the fifth day (Fig. 1f). For VIGS, two commonly used marker genes, protoporphyrin IX magnesium chelatase *subunit H (CrChlH)*, involved in chlorophyll biosynthesis [47], and phytoene desaturase (CrPDS), a key enzyme in the carotenoid biosynthetic pathway [48], were targeted to generate visible phenotypes. Seedlings or sprouts that were 2, 3, 4, and 5 days old were subjected to vacuum infiltration with Agrobacterium ( $OD_{600}=1.0$ ) harboring the TRV vectors for a duration of 30 min. Following the infiltration, the sprouts or seedlings were kept in the dark until they were 8-day-old and then exposed to light. A clear yellow phenotype was observed in cotyledons after silencing CrChlH, when the seedlings were first grown in the dark, followed by 2-3 days of light exposure. The cotyledons of the seedling infiltrated with the CrChlH-VIGS construct stayed yellow, whereas that of the control seedlings became green (Fig. 2a-b). Chlorophyll biosynthesis is light-regulated, and as expected, seedlings grown

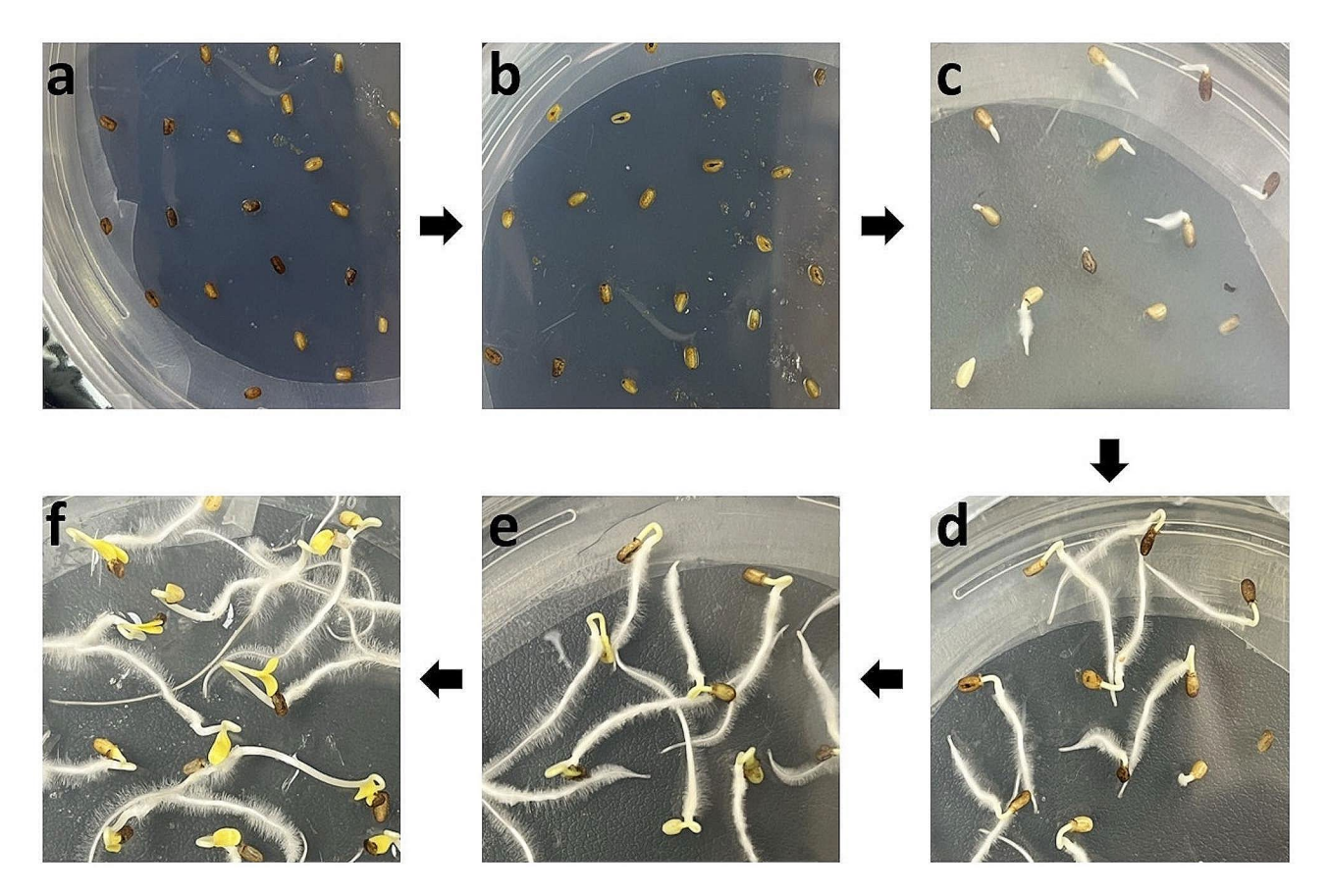
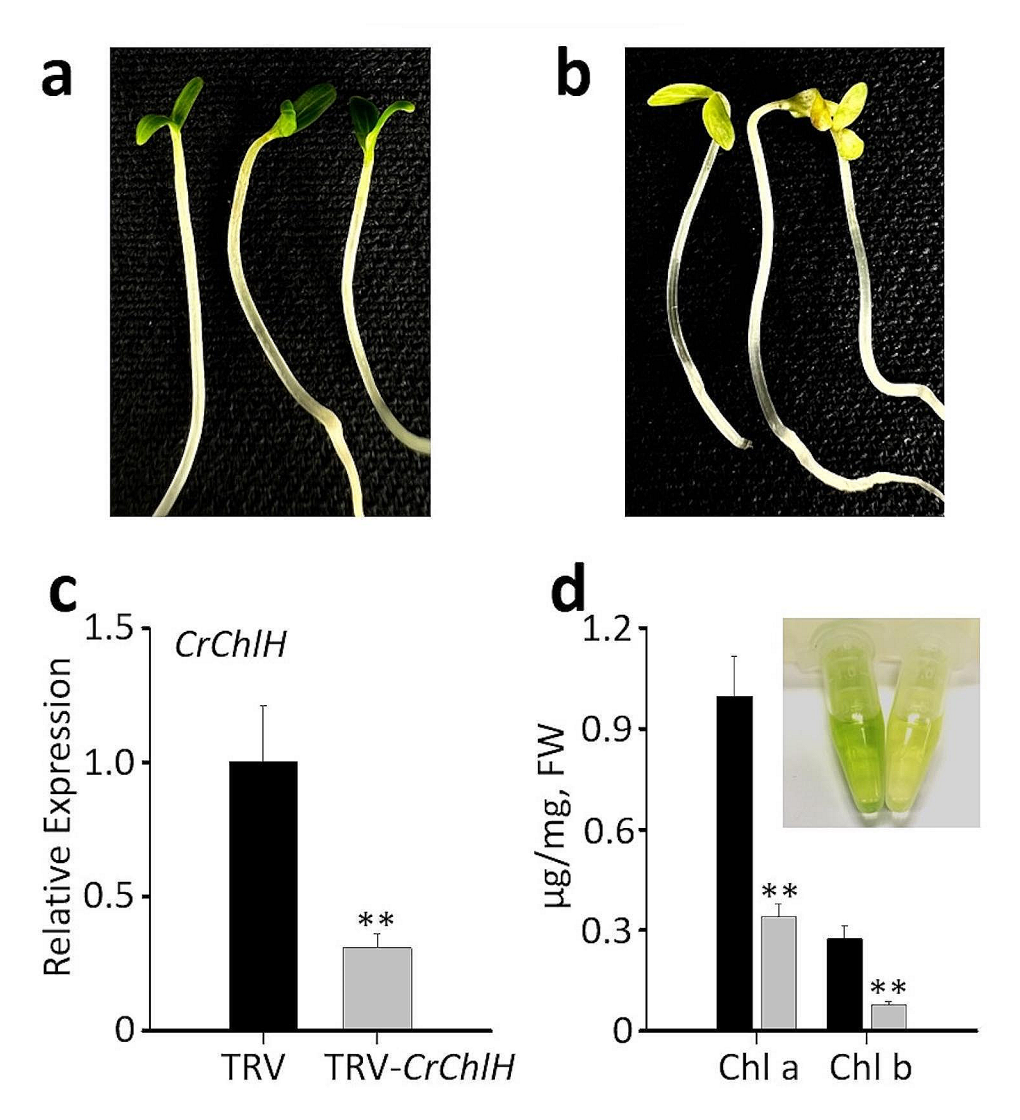


Fig. 1 Germination of *C. roseus* (cv. Little Bright Eye) seeds. Phenotype of *C. roseus* seeds/seedlings germinated on half-strength MS medium. **a-f**, the flow of seed germination from 0 (**a**) to 5 days (**f**) of growth

Liu et al. Plant Methods (2024) 20:26 Page 4 of 12



**Fig. 2** Cotyledon-VIGS of *CrChIH*. Phenotypes of the empty vector (TRV) control (**a**) and *CrChIH*-VIGS (TRV-*CrChIH*) (**b**) seedlings show the yellow cotyledons of *CrChIH*-VIGS seedlings. (**c**) Relative expression of *CrChIH* in control (TRV) and *CrChIH*-VIGS (TRV-*CrChIH*) cotyledons. (**d**) Concentrations of chlorophylls a (Chl a) and b (Chl b) in control (black) and *CrChIH*-VIGS (gray) cotyledons. Inserted picture shows the color difference of the chlorophyll solutions in the control (left) and TRV-*CrChIH* (right). *CrChIH* expression was measured using RT-qPCR. The *C. roseus RPS9* gene was used as an internal reference gene. The values represent means ±SD from three biological replicates. For each biological replicate, entire cotyledons were pooled from 8–9 seedlings (16–17 cotyledons). Statistical significance was calculated using Student's t test (\*\* *P* < 0.01)

in the dark rapidly accumulate chlorophyll after exposure to light. In our *ChlH* -VIGS study, it was difficult to visually observe the *yellow* phenotype in the light-grown seedlings (2 days of gemination in the dark followed by 3 days in light) even if the *ChlH* expression was significantly reduced (Additional file 1: Fig. S1a and 1b) because of the high chlorophyll content in the cells. Therefore, we carried out *ChlH*-VIGS in dark-grown seedlings initially (5 days in the dark) before exposing the seedlings to light. The decreased expression of *ChlH* prior to the light treatment yielded yellow cotyledons due to reduced chlorophyll accumulation. The *PDS* gene is often used as a marker in VIGS in many plant species including *C. roseus* [12]; however, we did not observe photobleaching

in the seedlings infiltrated with *CrPDS*, although *CrPDS* expression was reduced by approximately 70% in the cotyledons (Additional file 1: Fig. S1a and 1b). However, photobleaching was observed in the first pair of true leaves after the seedlings were transferred to soil (Additional file 1: Fig. S1c). The lack of phenotype in the cotyledon is possibly due to the age of the seedlings used in this study. *CrChlH* thus is a more suitable marker for cotyledon VIGS in plant species. The efficiency of silencing *CrChlH* was the highest (84%) when 5-day-old seedlings were used for infiltration (Table 1; Additional file 1: Fig. S2), indicating that complete emergence of the cotyledons from the seed coats is necessary for efficient *Agrobacterium* infection. To optimize the efficiency of

Liu et al. Plant Methods (2024) 20:26 Page 5 of 12

**Table 1** Optimization of cotyledon-VIGS of *CrChIH* in *C. roseus* using different time (days) and varying *Agrobacterium* concentration ( $OD_{600}$ ).

CONCENTIATION (OB600).	
Optimization	Yellow cotyledon
Parameter (day-OD <sub>600</sub> )	efficiency*
Set 1	
2d-1.0	3/50
3d-1.0	13/50
4d-1.0	24/50
5d-1.0	42/50
Set 2	
5d-0.2	26/50
5d-0.5	50/50
5d-1.0	37/50
5d-2.0	28/50

\*The efficiency is shown as the number of yellow cotyledons per 50 cotyledons. Data presented here are from three biological replicates. For each biological replicate, all cotyledons from 9 seedlings (18 cotyledons/replicate) were pooled to determine the phenotype

cotyledon-VIGS, different  ${\rm OD_{600}}$  values of the *Agrobacterium* infiltration solution were tested. The best result was achieved when the  ${\rm OD_{600}}$  value was at 0.5, resulting in 100% efficiency (Table 1). This optimized condition was then used for subsequent VIGS experiments in *C. roseus*.

To confirm the silencing of CrChlH through cotyledon-VIGS, CrChlH expression in cotyledons was measured using reverse transcription quantitative PCR (RT-qPCR). As expected, the expression of CrChlH was reduced by 70% in the CrChlH-VIGS cotyledons compared to the control (Fig. 2c). In addition, the contents of chlorophyll a (Chla) and chlorophyll b (Chlb) were decreased in CrChlH-VIGS cotyledons (Fig. 2d). These results confirmed that the yellow phenotype of the cotyledons was due to the reduction in chlorophyll contents resulted from silencing CrChlH. To further determine the CrChlH-VIGS phenotype in the first pair of true leaves and subsequent development, we grew the seedlings in soil. However, only about 20% of the plants showed the yellow phenotype in the first pair of true leaves (Additional file 1: Fig. S3a), and the following pair of leaves did not show the phenotype (Additional file 1: Fig. S3b). The results suggest that the virus cannot spread efficiently to the newly emerged leaves in C. roseus.

#### Cotyledon-VIGS of CrGATA1 in C. roseus

The sequential conversion of tabersonine to vindoline is catalyzed by seven genes encoding enzymes tabersonine 16-hydroxylase 2 (T16H2), 16-hydroxytabersonine *O*-methyltransferase (16OMT), tabersonine 3-oxygenase (T3O), tabersonine 3-reductase (T3R), 3-hydroxy-16-methoxy-2,3-dihydrotabersonine *N*-methyltransferase (NMT), desacetoxyvindoline-4-hydroxylase (D4H), and deacetylvindoline-4-*O*-acetyltransferase (DAT) [49] (Fig. 3a). In our previous study, we have

demonstrated that the expression of CrGATA1, a positive regulator of vindoline biosynthesis, can be effectively knocked down using the pinch wounding VIGS method. VIGS of *CrGATA1* reduced the expression of *T3O*, *T3R*, and DAT [13]. In this study, we further validated the applicability of cotyledon-VIGS in C. roseus by targeting CrGATA1. Five-day-old C. roseus seedlings (germinated in dark for 2 days followed by 3 days of light) were vacuum-infiltrated and then incubated in dark for 3 days and in light for another 3 days. The conditions for growing C. roseus seedlings used for silencing TIA related genes were different from those used for CrChlH-VIGS. This is because TIA biosynthesis (especially vindoline) requires light (darkness inhibits vindoline production). The expression of CrGATA1 reduced by approximately 70% in CrGATA1-VIGS cotyledons (Fig. 3b). Consistent with our previous findings [13], the expression of the vindoline pathway genes, T3O, T3R, and DAT, was significantly downregulated in the CrGATA1-VIGS cotyledons (Fig. 3c). Furthermore, we detected a decrease of vindoline and an increase of tabersonine, the precursor of vindoline synthesis, in the CrGATA1-VIGS cotyledons (Fig. 3d), which is in agreement with our previous results using the pinch wounding VIGS method [13]. These results further validate the application of cotyledon-VIGS in C. roseus for functional characterization of the pathway genes.

#### Cotyledon-VIGS of CrMYC2 combined with MeJA treatment

CrMYC2 is a component of jasmonate signaling and a key regulator of the TIA pathway. In our cotyledon-VIGS experiments, expression of CrMYC2 was knocked down by 90% (Fig. 4a). However, only ORCA3 showed a 40% reduction in expression, whereas ORCA2 expression was higher in CrMYC2-VIGS cotyledons compared to the control (Fig. 4a). Subsequently, we treated the CrMYC2-VIGS cotyledons with 100 µM MeJA for 2 h before collecting samples. The results showed that both ORCA2 and ORCA3 were significantly downregulated upon CrMYC2 silencing, with ORCA3 showing an 80% reduction compared to the 40% reduction without MeJA treatment (Fig. 4b). In *C. roseus*, the expression of *CrMYC2*, ORCA2, and ORCA3 is induced by MeJA, and CrMYC2 is essential for MeJA-responsive expression of ORCAs [34]. In addition, other factors, such as AT-hook proteins, are known to regulate ORCA expression [50]. In the absence of MeJA, minimum expression of *CrMYC2* in VIGS seedlings had little to no significant effect on the expression of ORCA2 and ORCA3. Our results agreed with the previously published findings [34] showing that without MeJA treatment, RNAi-mediated silencing of CrMYC2 in C. roseus cell lines has no significant effect on the expression of ORCA2 and ORCA3; however, MeJA treatment significantly affected the expression of ORCA2

Liu et al. Plant Methods (2024) 20:26 Page 6 of 12

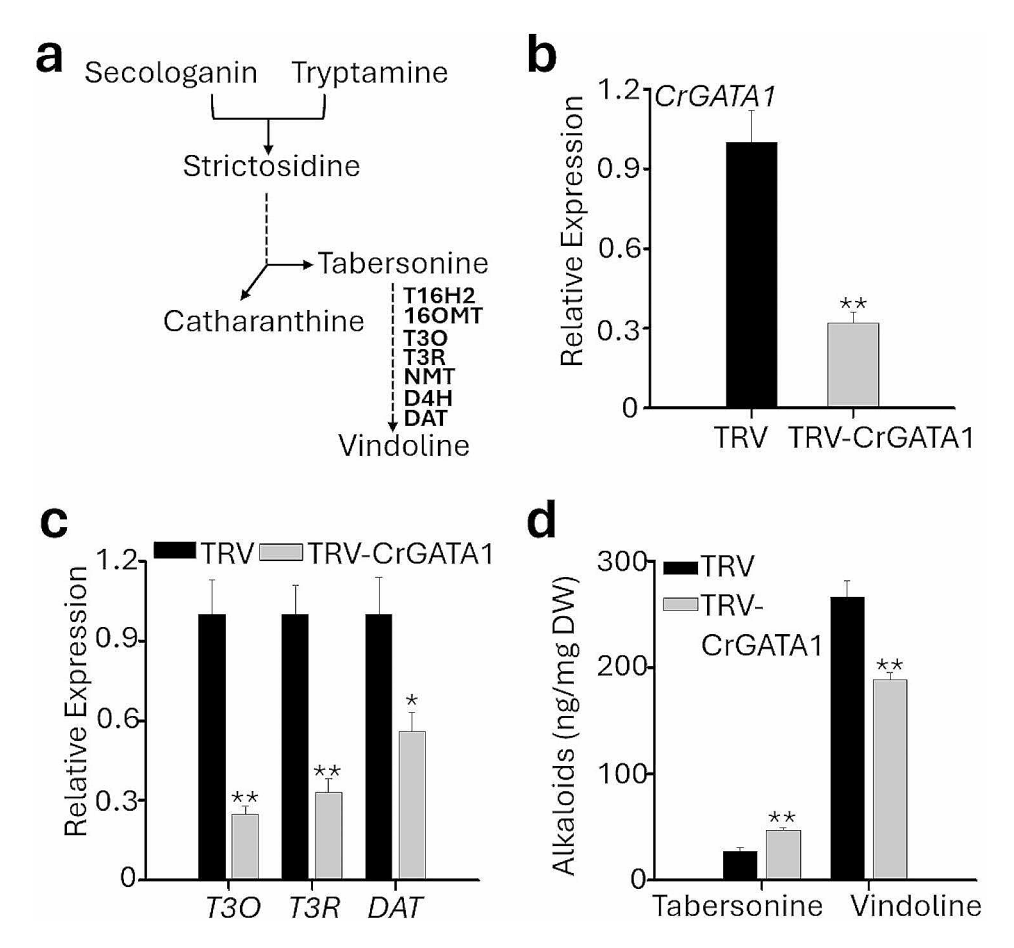


**Fig. 3** Cotyledon-VIGS of *CrGATA1*. (**a**) A shematic diagram showing vindoline biosynthetic pathway in *C. roseus*. T16H2, tabersonine 16-hydroxylase 2; 16OMT, 16-hydroxytabersonine *O*-methyltransferase; T3O, tabersonine 3-oxygenase; T3R, tabersonine 3-reductase; NMT, 3-hydroxy-16-methoxy-2,3-dihydrotabersonine *N*-methyltransferase; D4H, desacetoxyvindoline-4-hydroxylase; DAT, deacetylvindoline-4-*O*-acetyltransferase. (**b**) Relative expression of *CrGATA1* in empty vector control (TRV) and *CrGATA1*-VIGS (TRV-*CrGATA1*) cotyledons. (**c**) Relative expression of *T3O*, *T3R* and *DAT* in the control and *CrGATA1*-VIGS cotyledons. Gene expression was measured using RT-qPCR, and the *C. roseus RPS9* gene was used as an internal reference gene. Alkaloids were extracted and analyzed by LC-MS/MS, and the concentrations of the alkaloids were estimated based on peak areas compared with standards. DW, dry weight. The values represent means ± SD from three biological replicates. For each biological replicate, entire cotyledons were pooled from 8–9 seedlings (16–17 cotyledons). Statistical significance was calculated using Student's t test (\* *P* < 0.05 and \*\* *P* < 0.01). The *black* and *qrey* bars represent the TRV (empty vector control) and TRV-*CrGATA1*, respectively

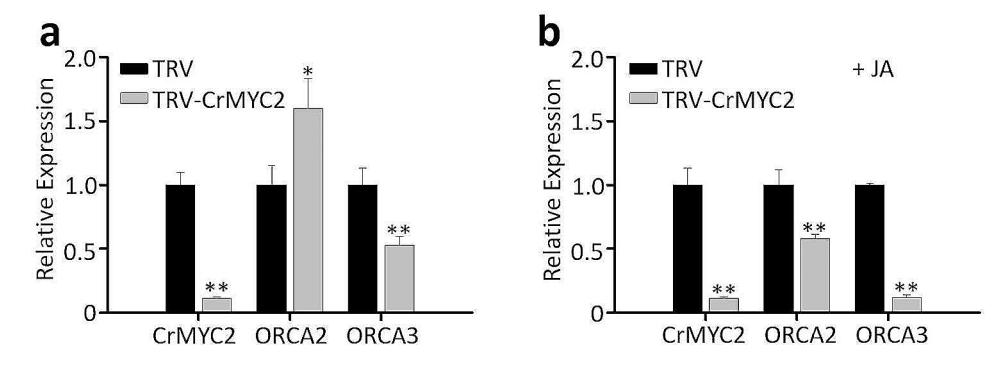


**Fig. 4** Cotyledon-VIGS of *CrMYC2* with or without MeJA treatment. Relative expression of *CrMYC2*, *ORCA2*, and *ORCA3* in empty vector control (TRV) and *CrMYC2*-VIGS (TRV-*CrMYC2*) cotyledons without (**a**) or with (**b**) MeJA treatment (+ MeJA; 100  $\mu$ M). MeJA (100  $\mu$ M) was added to the petri dishes containing the seedlings and petri dishes covered with the lids for 2 h. Gene expression was measured using RT-qPCR. The *C. roseus RPS9* gene was used as an internal reference gene. The values represent means  $\pm$  SD from three biological replicates. For each biological replicate, entire cotyledons were pooled from 8–9 seedlings (16–17 cotyledons). Statistical significance was calculated using Student's t test (\*\* P < 0.01)

Liu et al. Plant Methods (2024) 20:26 Page 7 of 12

and *ORCA3* compared to control. Additionally, our findings suggest that when conducting cotyledon-VIGS in *C. roseus*, the seedlings are amenable to other treatments, such as other phytohormones or stress conditions, providing opportunities for further investigations.

# Simultaneous VIGS of CrGBF1/2 and overexpression of CrMYC2

Previous studies have established a seedling-based transient overexpression method for C. roseus using vacuum infiltration [51]. Here, we aimed to explore the possibility of simultaneously achieving gene silencing and transient gene overexpression in *C. roseus* seedlings. CrGBF1/2 are negative regulators of TIAs biosynthesis, and CrMYC2 works antagonistically with CrGBF1/2 to regulate TIAs biosynthesis [35]. We hypothesized that overexpression of CrMYC2 while silencing CrGBF1/2 would maximize the levels of TIA biosynthesis. For cotyledon-VIGS, gene fragments of CrGBF1 and CrGBF2 were fused to achieve simultaneous silencing of both genes. The Agrobacterium solutions for GBF1/2-VIGS and CrMYC2-overexpression (OE) were mixed in an equal proportion prior to vacuum infiltration. Five-day-old seedlings (germinated in dark for 2 days then kept in light for 3 days) were used for Agrobacterium-infiltration, and the resulting seedlings were kept in the dark for 3 days and then in light for another 3 days before measuring gene expression. Our results showed that CrMYC2 was overexpressed by 8-fold, while CrGBF1/2 were knocked down by 60-70% in VIGS+OE seedlings (Fig. 5a). Tryptophan decarboxylase (TDC) and strictosidine synthase (STR), two enzymes in the TIA pathway, are the targets of CrMYC2 and CrGBF1/2. Tryptophan is decarboxylated by TDC to produce tryptamine, the indole moiety of TIA. Condensation of tryptamine with the terpenoid moiety secologanin to produce the first TIA, strictosidine, is catalyzed by STR [52]. The expression of *TDC* and *STR* was induced significantly (4–6 fold) in the VIGS+OE cotyledons (Fig. 5a). However, *TDC* expression was induced moderately (2-fold) whereas that of *STR* was repressed when only CrMYC2 was overexpressed (Fig. 5b). The expression of *MYC2* increased 8-fold in VIGS+OE seedlings compared to control whereas it increased 5-fold in *MYC2*-OE seedlings (Fig. 5a and b). This difference in *MYC2* expression could possibly be the effect of silencing of the GBFs in VIGS+OE seedlings. These findings suggest that the cotyledon-VIGS method can be combined with transient gene overexpression to achieve simultaneous up- and down-regulation of desired genes in *C. roseus*.

#### Application of cotyledon-VIGS in G. inflata and A. annua

The success of cotyledon-VIGS in *C. roseus* prompted us to apply this method to other plants including G. inflata and A. annua, two important medicinal plants. We initially used the conditions that worked well for C. roseus (30 min infiltration with  $OD_{600}$  0.5 Agrobacterium solution). However, silencing efficiency was low for G. inflata possibly because the cotyledons are very thick. Therefore, for G. inflata, the infiltration time was increased to 60 min and the concentration of infiltration solution was increased to  $OD_{600} = 1.0$  to achieve the best efficiency (Table 2). In contrast, A. annua seedlings are sensitive to long exposure (i.e. 30 min) to Agrobacterium infiltration. We thus reduced the infiltration time to 10 min for A. annua (Table 2). Six to seven-day-old seedlings germinated in dark were used for VIGS. The respective *ChlH* genes were used for cotyledon-VIGS in both plants, and we observed yellow-colored cotyledons with 100% efficiency (Table 2; Fig. 6a and d), which was confirmed by measuring the chlorophyll concentration and gene expression (Fig. 6b, c, e and f). Based on these results, we conclude that cotyledon-VIGS is a promising and generally applicable technique for investigating gene function in plants.

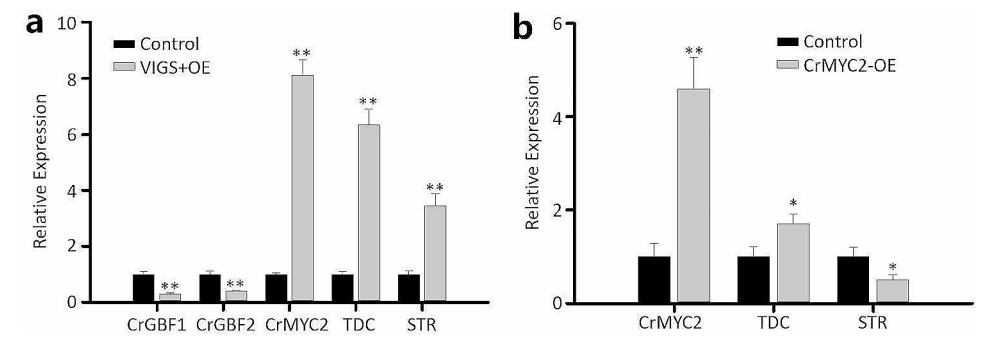


**Fig. 5** Cotyledon-VIGS of *CrGBF1/GBF2* and overexpression of *CrMYC2*. (a) Relative expression of *CrGBF1*, *CrGBF2*, *CrMYC2*, *TDC* and *STR* in empty vector control (TRV) and *CrGBF1/GBF2/MYC2* cotyledons. (b) Relative expression of *CrMYC2*, *TDC* and *STR* in empty vector control and *CrMYC2* overexpression cotyledons. Relative expression was measured by RT-qPCR, and the *C. roseus RPS9* gene was used as an internal reference gene. The values represent means ± SD from three biological replicates. For each biological replicate, entire cotyledons were pooled from 8–9 seedlings (16–17 cotyledons). Statistical significance was calculated using Student's t test (\*\* P < 0.01)

Liu et al. Plant Methods (2024) 20:26 Page 8 of 12

**Table 2** Optimized conditions of the cotyledon-VIGS in two medicinal plants

Plants/Conditions	Glycyrrhiza inflata	Arte- misia annua
Seedling age (days)	7	6
Infiltration time (minutes)	60	10
OD <sub>600</sub> of infiltration solution	1.0	0.5
Efficiency*	30/30	50/50

<sup>\*</sup>After infiltration with the VIGS vectors, the seedlings were incubated for 6 days (3 days in dark and then 3 days in 16 h light /8 h dark regime), to record yellow cotyledon phenotype. The efficiency is shown as the number of yellow cotyledons per 30–50 cotyledons

#### Discussion

VIGS is a valuable tool for plant functional genomics and has been extensively used to decipher the gene functions in developmental and metabolic pathways [1-3, 12,13, 15]. VIGS is especially useful for non-model plant species for which the generation of stable transgenic plants is often challenging [1]. To enhance the applicability of VIGS, various infiltration methods have been developed, among which the sprout vacuum infiltration (SVI) method allows for high-throughput gene function analysis [25]. SVI-based VIGS and other seed-based infiltration methods [10, 18] are rapid and the bleaching phenotype is usually easy to observe in the first pair of true leaves. However, for plants with a prolonged developmental period, the application of SVI method is more time consuming. For C. roseus, the first pair of true leaves appear 3 weeks after germination [51]. The cotyledon-VIGS method (Fig. 2) circumvents this issue and maximizes the efficiency of the VIGS. In our laboratory, 5-day-old C. roseus seedlings were used for Agrobacterium-infiltration and samples were ready for collection 6

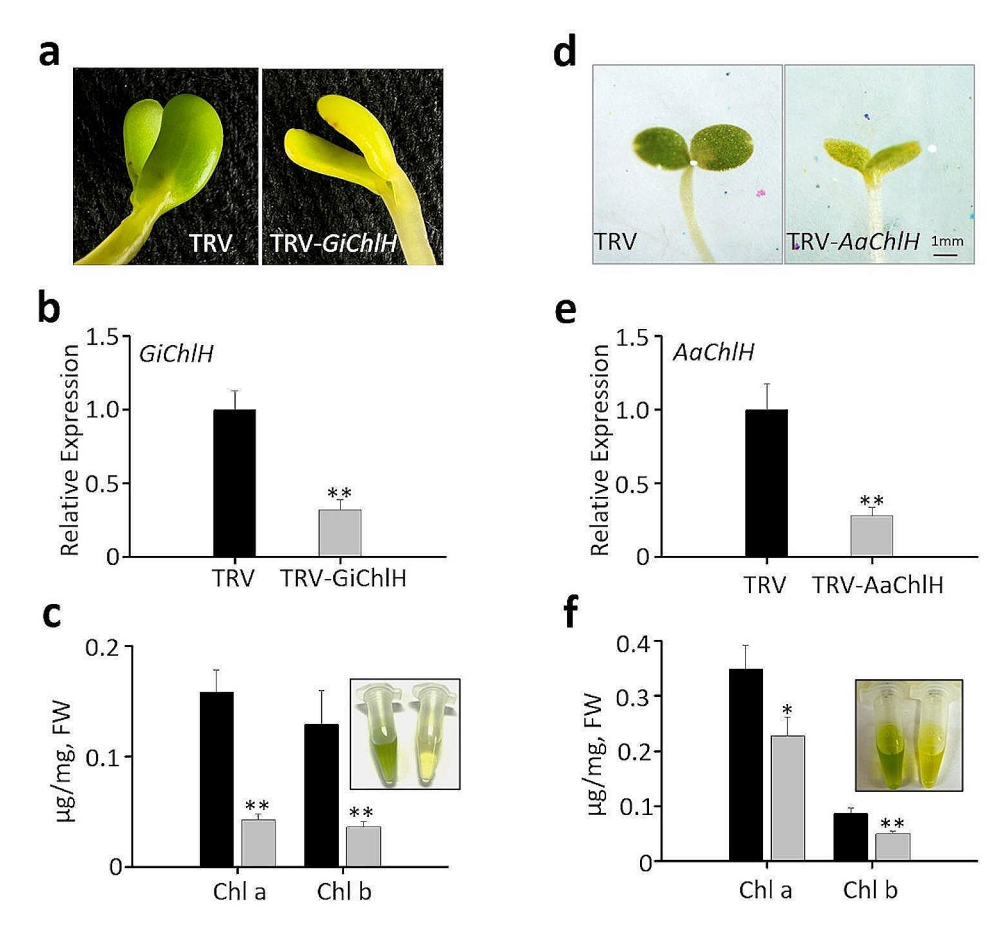


**Fig. 6** Cotyledon-VIGS of *ChIH* genes in *G. inflata* and *A. annua*. (a) Phenotypes of empty vector control (TRV) and *GiChIH*-VIGS (TRV-*GiChIH*) seedlings. (b) Relative expression of *GiChIH* in the control and *GiChIH*-VIGS cotyledons. (c) Concentration of chlorophylls a (ChI a) and b (ChI b) in the control and *GiChIH*-VIGS cotyledons. (d) Phenotypes of TRV control and *AaChIH*-VIGS (TRV-*AaChIH*) seedlings. (e) Relative expression of *AaChIH*-In the control and *AaChIH*-VIGS cotyledons. (f) Concentration of ChI a and ChI b in control and *AaChIH*-VIGS cotyledons. In a and d, the yellow cotyledons of the VIGS seedlings are consistent with the chlorophyll extractions showing in the inserts of c and f (Left, TRV control; right, *ChIH*-VIGS). Relative expression was measured using RT-qPCR, and the *A. annua* and *G. inflata Actin* genes were used as an internal reference. The values represent means ± SD from three biological replicates. For each biological replicate, entire cotyledons were pooled from 8–9 seedlings (16–17 cotyledons) for *A. annua*, and 4–5 seedlings (8–10 cotyledons) for *G. inflata*. Statistical significance was calculated using Student's t test (\* *P* < 0.05 and \*\* *P* < 0.01)

Liu et al. Plant Methods (2024) 20:26 Page 9 of 12

days after infiltration. Moreover, cotyledon-VIGS retains the high-throughput advantage of SVI. The efficiency of VIGS varies for each individual gene. The silencing efficiency of genes varies from 60 to 90% in our study (Figs. 3, 4, 5 and 6).

Previous studies have reported varying efficiency of different infiltration methods in different plant species. For instance, while SVI has been highly effective in certain Solanaceous crops, such as tomato and eggplant [25], its efficiency in two Goji species (Lycium species), which also belong to *Solanaceae*, is notably lower [28]. The pinch wounding method has been found to be suitable for *C. roseus* [11]; however, its efficiency is difficult to determine, leading to the development of an improved method in which the marker gene CrPDS is simultaneously silenced with the target gene to visualize the gene silencing effect [16]. The inconsistency in silencing may be attributed to the requirement of the virus to spread through vascular tissue to the distant plant tissues. We found that the VIGS efficiency greatly declined in the newly emerged leaves (Additional file 1: Fig. S3). In contrast, cotyledon-VIGS does not necessitate long-distance viral spread, making it highly efficient in diverse plant species. We demonstrated 100% efficiency in cotyledon-VIGS for C. roseus, G. inflata, and A. annua (Tables 1 and 2), suggesting its potential as a general and efficient VIGS method for most plant species.

C. roseus accumulates two valuable anti-cancer agents, vinblastine and vincristine, specifically in leaves, with catharanthine and vindoline being their direct precursors. Understanding the regulatory mechanisms underlying the biosynthesis of catharanthine and vindoline can serve as a foundation for improving vinblastine and vincristine production. Although vinblastine and vincristine are not accumulated in the cotyledon of C. roseus, catharanthine and vindoline are readily produced [53]. Cotyledon-VIGS of CrGATA1 reiterated the positive effects of CrGATA1 in regulating vindoline biosynthesis (Fig. 3). Additionally, CrMYC2 and its targets, ORCAs, act as general regulators of catharanthine and most tryptamine-derived indole alkaloids upstream of vindoline [34]. Cotyledon-VIGS of CrMYC2, followed by JA treatment, further validated the effects of CrMYC2 on its target genes and the involvement of the JA signaling (Fig. 4). Therefore, cotyledon-VIGS provides a platform for investigating the regulatory mechanisms of catharanthine and vindoline, as well as other upstream TIAs.

The combination of cotyledon-VIGS with transient overexpression in *C. roseus* seedlings allows for investigating the relationship between multiple factors in a pathway, even in non-model plants where stable transformation is challenging. By overexpressing the activator *CrMYC2* and simultaneously knocking down two repressors, *CrGBF1* and *CrGBF2*, using cotyledon-VIGS, we

observed a greater upregulation of *TDC* and *STR* compared to control and the individual gene manipulation (Fig. 5).

Cotyledon-VIGS overcomes several issues facing the previously established VIGS methods and can be used for other non-model plant species. Although a protocol optimized for one species might work for other species, the parameters still need to be fine-tuned for each plant species to achieve optimal results. Each plant species is different with respect to germination time, size, and morphology of the cotyledon, as well as the sensitivity to Agrobacterium infection. In our study, the parameters that worked well for C. roseus did not yield the best results for G. inflata and A. annua. Therefore, certain conditions, such as age of the seedling, density  $(OD_{600})$  of Agrobacterium-suspension, and infiltration time, should be optimized for each plant species to achieve optimal results. It is reasonable to suggest cotyledon-VIGS as a general platform for gene silencing and investigation of the synergistic effects of multiple genes. Cotyledon-VIGS is most effective in studying genes that are expressed in early development. Nonetheless, we were also able to obtain cotyledon-VIGS C. roseus plants that developed true leaves, making the system potentially useful for studying late stage-expressed genes.

#### **Methods**

#### Plant materials and growth conditions

Seeds of *C. roseus* (cultivar 'Little Bright Eye'; obtained from NESeed, USA) were used in this study. The seeds were surface sterilized using 75% ethanol for 5 min and then 30% sodium hypochlorite solution (Sigma-Aldrich) for 10 min. After rinsing with sterile ddH<sub>2</sub>O for 5 times, the seeds were inoculated on half-strength Murashige and Skoog (½ MS) medium. The seeds were kept in the dark at 30 °C for two days and then transferred to an incubator at 26 °C. For VIGS experiments targeting the *CrChlH* (accession numbers HQ608936) and *CrPDS* (accession number JQ655739) in *C. roseus*, the germinated seeds were grown in the dark for another 3 days. However, for VIGS of TIA pathway genes, the germinated seeds were grown under a light regime of 16/8 photoperiod for 3 days.

For VIGS of *ChlH* genes in *G. inflata*, and *A. annua*, the seeds of respective species were germinated on half-strength MS medium, and seedlings were grown in the dark at 26  $^{\circ}$ C. Seeds of *G. inflata* were treated with  $\rm H_2SO_4$  for 30 min [46], surface sterilized with 30% sodium hypochlorite solution (Sigma-Aldrich) for 10 min, and germinated on half-strength MS medium for 7 days in dark. Seeds of *A. annua* were surface sterilized as described for *C. roseus* seeds and germinated on half-strength MS medium for 6 days in dark.

Liu et al. Plant Methods (2024) 20:26 Page 10 of 12

#### Plasmid construction and Agrobacterium transformation

The primers used for plasmid construction are listed in Additional file 1: Table S1 and the vectors are schematically presented in Additional file 1: Figure S4. For VIGS vectors, fragments of target genes were amplified with primers containing KpnI and XhoI restriction enzyme recognition sites and inserted into the multiple cloning sites (MCS) of pTRV2 [9]. Fragments of CrGBF1 (accession numbers AF084971) and CrGBF2 (accession numbers AF084972) were fused together using primers with overlapping sequences. The VIGS vectors for silencing CrChlH, CrPDS [12], CrGATA1 [13], and overexpressing CrMYC2 (accession number AF283507) [35] have been described previously. The ChlH gene sequences of G. *inflata* and *A. annua* were obtained from an unpublished G. inflata transcriptome and a published A. annua transcriptome [54], respectively (Additional file 1: Supplementary text).

Agrobacterium tumefaciens strain GV3101 competent cells stored at -80 °C were thawed on ice and then mixed with 500 ng of recombined plasmids. The mixture was kept on ice for 30 min and then rapidly frozen in liquid nitrogen for 30 s, followed by incubation at 37 °C for 5 min. The cells were returned to ice for 5 min and quenched with 500  $\mu L$  of fresh Luria Broth (LB) liquid medium. Following incubation in a shaker at 28 °C and 200 rpm for 2.5 h, 100  $\mu L$  of cells were plated onto LB agar plates containing rifampicin (30 mg/L) and kanamycin (100 mg/L) and incubated at 28 °C for 3 days.

#### Agrobacterium culture and preparation of infiltration

A single positive colony of transformed Agrobacterium was inoculated into 1 mL of LB liquid medium containing 30 mg/L rifampicin and 100 mg/L kanamycin, followed by overnight culturing in a shaker at 28 °C with a speed of 200 rpm. Subsequently, 100 µL of Agrobacterium cells were transferred into 10 mL of fresh LB liquid medium supplemented with the aforementioned antibiotics and cultured overnight at 28 °C with a speed of 200 rpm. The Agrobacterium cultures were then centrifuged at 6000 g for 5 min, and the resulting pellet was resuspended in an infiltration buffer containing 10 mM MgCl<sub>2</sub>, 10 mM MES, and 100 μM acetosyringone, at a desired OD<sub>600</sub> (optical density at 600 nm). The suspension was then incubated at 28 °C for at least 3 h. Afterward, the infiltration solution was mixed with Silwet L-77 at a concentration of 0.01% `and was ready for infiltration. For simultaneous VIGS+OE (overexpression), Agrobacterium harboring the CrGBF-VIGS and CrMYC2-OE constructs were mixed in equal proportions before infiltration.

#### Infiltration of the seedlings

Sprouts or seedlings of *C. roseus*, *G. inflata*, and *A. annua* were immersed in the infiltration solution in either a 15

mL or 50 mL tube. The opening of the tube was covered with parafilm that was punctured to produce small holes to allow for air exchange. For VIGS of the ChlH or PDS gene, the tubes were wrapped with aluminum foil to prevent light exposure (Additional file 1: Figure S5a) and placed in a vacuum chamber. The infiltration was carried out at the desired pressure of 20 kPa and for the appropriate duration (Additional file 1: Figure S5b). Afterward, the pressure was slowly released. Sprouts or seedlings were gently taken out from the tubes, washed with sterile distilled water for five times, and placed on petri dishes with autoclaved wet filter papers. The seedlings were then kept in the dark at 26 °C for 3 days, followed by transferring to light (15–20  $\mu$ mol m<sup>-2</sup> s<sup>-1</sup>; photoperiod 16/8) for 3 days. For VIGS of the ChlH gene, cotyledons were harvested for chlorophyll content determination and RNA isolation, or the seedlings were transferred to soil for further observation. For VIGS of CrMYC2, infiltrated C. roseus seedlings were treated with 100 µM MeJA for 2 h 6 days after infiltration. For VIGS of CrGATA1, infiltrated *C. roseus* seedlings were kept in the dark for 3 days and then in 16 h light/8 h dark for another 3 days. The cotyledons were then collected for gene expression and metabolite analysis.

#### **Determination of chlorophyll contents**

The protocol for chlorophyll content determination has been previously described [55]. Briefly, samples were weighed and placed in 1 mL of dimethyl-formamide (DMF) and kept in the dark at 4 °C overnight. Optical density at 664 nm and 647 nm (A<sub>664</sub> and A<sub>647</sub>) was measured using a spectrophotometer, using pure DMF as a blank. The contents of chlorophyll a ( $C_a$ ) and chlorophyll b ( $C_b$ ) were calculated using the following formulas:  $C_a$  = 11.65×A<sub>664</sub> – 2.69×A<sub>647</sub>;  $C_b$  = 20.81×A<sub>647</sub> – 4.53×A<sub>664</sub>.

#### RNA isolation, cDNA synthesis, and RT-qPCR

Total RNA was extracted from C. roseus VIGS cotyledons using the RNeasy Plant Mini Kit according to the manufacturer's instructions (QIAGEN, United States). Approximately 2 µg of total RNA was treated with DNase I to remove contaminating genomic DNA. First-strand cDNA synthesis was carried out using Superscript III reverse transcriptase (Invitrogen, United States) in a total reaction volume of 20 µL. Reverse transcription quantitative PCR (RT-qPCR) was performed to measure the transcript levels of target genes. CrRPS9 was used as an internal control for normalization [40]. AaActin and GiActin were used as internal control for A. annua and G. inflata, respectively. Relative gene expression was determined as previously described [13]. All RT-qPCRs were performed in triplicate and repeated twice to ensure accuracy and reproducibility. The primer sequences used for RT-qPCR are provided in Additional file 1: Table S1.

Liu et al. Plant Methods (2024) 20:26 Page 11 of 12

#### Alkaloid extraction and analysis

Extraction and analysis of alkaloids from *C. roseus* VIGS cotyledons were performed as described previously [13]. The concentrations of the alkaloids were calculated using a standard curve.

#### **Supplementary Information**

The online version contains supplementary material available at https://doi.org/10.1186/s13007-024-01154-x.

Supplementary Material 1

#### Acknowledgements

We would like to thank Dr. Bert Lynn for assistance in determining the alkaloids' concentration.

#### Author contributions

LY and SP designed the study. YL, RL, BP, and JS performed the experiments. YL wrote the manuscript. All authors read, edited and approved the final manuscript.

#### **Funding**

This work is supported partially by the Harold R. Burton Endowed Professorship to L.Y.

#### Data availability

All data generated or analyzed during this study are included in this published article (and its supplementary information files).

#### **Declarations**

#### Ethics approval and consent to participate

Not applicable.

#### Consent for publication

All authors read and approved the manuscript.

#### **Competing interests**

The authors declare no competing interests.

#### **Author details**

<sup>1</sup>Department of Plant and Soil Sciences and Kentucky Tobacco Research and Development Center, University of Kentucky, Lexington, KY 40546, USA

Received: 31 July 2023 / Accepted: 6 February 2024 Published online: 12 February 2024

#### References

- 1. Jagram N, Dasgupta I. Principles and practice of virus induced gene silencing for functional genomics in plants. Virus Genes. 2023;59(2):173–87.
- Rossner C, Lotz D, Becker A. VIGS goes viral: how VIGS transforms our understanding of Plant Science. Annu Rev Plant Biol. 2022;73:703–28.
- Dommes AB, Gross T, Herbert DB, Kivivirta KI, Becker A. Virus-induced gene silencing: empowering genetics in non-model organisms. J Exp Bot. 2019;70(3):757–70.
- Courdavault V, Besseau S, Oudin A, Papon N, O'Connor SE. Virus-Induced Gene silencing: hush genes to make them talk. Trends Plant Sci. 2020;25(7):714–5.
- Liu E, Page JE. Optimized cDNA libraries for virus-induced gene silencing (VIGS) using tobacco rattle virus. Plant Methods. 2008;4:1–13.
- Ratcliff F, Martin-Hernandez AM, Baulcombe DC. Technical advance: tobacco rattle virus as a vector for analysis of gene function by silencing. Plant J. 2001;25(2):237–45.

- Shi G, Hao M, Tian B, Cao G, Wei F, Xie Z. A methodological advance of Tobacco Rattle Virus-Induced Gene silencing for Functional Genomics in plants. Front Plant Sci. 2021;12:671091.
- Burch-Smith TM, Schiff M, Liu Y, Dinesh-Kumar SP. Efficient virus-induced gene silencing in Arabidopsis. Plant Physiol. 2006;142(1):21–7.
- 9. Liu Y, Schiff M, Dinesh-Kumar S. Virus-induced gene silencing in tomato. Plant J. 2002;31(6):777–86.
- Zhang J, Yu D, Zhang Y, Liu K, Xu K, Zhang F, Wang J, Tan G, Nie X, Ji Q.
   Vacuum and co-cultivation agroinfiltration of (germinated) seeds results in tobacco rattle virus (TRV) mediated whole-plant virus-induced gene silencing (VIGS) in wheat and maize. Front Plant Sci. 2017;8:393.
- Liscombe DK, O'Connor SE. A virus-induced gene silencing approach to understanding alkaloid metabolism in Catharanthus roseus. Phytochemistry. 2011;72(16):1969–77.
- Patra B, Liu Y, Singleton JJ, Singh SK, Pattanaik S, Yuan L. Virus-Induced Gene Silencing as a Tool to study regulation of Alkaloid Alkaloids Biosynthesis in Medicinal plants Medicinal plants. Plant secondary Metabolism Engineering: methods and protocols. Springer; 2022. pp. 155–64.
- Liu Y, Patra B, Pattanaik S, Wang Y, Yuan L. GATA and phytochrome interacting factor transcription factors regulate light-induced vindoline biosynthesis in Catharanthus roseus. Plant Physiol. 2019;180(3):1336–50.
- Payne RM, Xu D, Foureau E, Teto Carqueijeiro MI, Oudin A, Bernonville TD, Novak V, Burow M, Olsen CE, Jones DM, et al. An NPF transporter exports a central monoterpene indole alkaloid intermediate from the vacuole. Nat Plants. 2017;3:16208.
- Patra B, Pattanaik S, Schluttenhofer C, Yuan L. A network of jasmonateresponsive bHLH factors modulate monoterpenoid indole alkaloid biosynthesis in Catharanthus roseus. New Phytol. 2018;217(4):1566–81.
- Yamamoto K, Grzech D, Koudounas K, Stander EA, Caputi L, Mimura T, Courdavault V, O'Connor SE. Improved virus-induced gene silencing allows discovery of a serpentine synthase gene in Catharanthus roseus. Plant Physiol. 2021;187(2):846–57.
- Agarwal AV, Singh D, Dhar YV, Michael R, Gupta P, Chandra D, Trivedi PK. Virusinduced silencing of key genes leads to differential impact on withanolide biosynthesis in the medicinal plant, Withania somnifera. Plant Cell Physiol. 2018;59(2):262–74.
- Zhang J, Wang F, Zhang C, Zhang J, Chen Y, Liu G, Zhao Y, Hao F, Zhang J. A novel VIGS method by agroinoculation of cotton seeds and application for elucidating functions of GhBl-1 in salt-stress response. Plant Cell Rep. 2018;37:1091–100.
- Ryu CM, Anand A, Kang L, Mysore KS. Agrodrench: a novel and effective agroinoculation method for virus-induced gene silencing in roots and diverse solanaceous species. Plant J. 2004;40(2):322–31.
- 20. Chen J-C, Jiang C-Z, Gookin T, Hunter D, Clark D, Reid M. Chalcone synthase as a reporter in virus-induced gene silencing studies of flower senescence. Plant Mol Biol. 2004;55:521–30.
- 21. Fu DQ, Zhu BZ, Zhu HL, Jiang WB, Luo YB. Virus-induced gene silencing in tomato fruit. Plant J. 2005;43(2):299–308.
- Qu J, Ye J, Geng Y-F, Sun Y-W, Gao S-Q, Zhang B-P, Chen W, Chua N-H. Dissecting functions of KATANIN and WRINKLED1 in cotton fiber development by virus-induced gene silencing. Plant Physiol. 2012;160(2):738–48.
- Tian J, Pei H, Zhang S, Chen J, Chen W, Yang R, Meng Y, You J, Gao J, Ma N. TRV-GFP: a modified Tobacco rattle virus vector for efficient and visualizable analysis of gene function. J Exp Bot. 2014;65(1):311–22.
- Ekengren SK, Liu Y, Schiff M, Dinesh-Kumar S, Martin GB. Two MAPK cascades, NPR1, and TGA transcription factors play a role in Pto-mediated disease resistance in tomato. Plant J. 2003;36(6):905–17.
- 25. Yan H-x, Fu D-q, Zhu B-z, Liu H-p. Shen X-y, Luo Y-b: sprout vacuum-infiltration: a simple and efficient agroinoculation method for virus-induced gene silencing in diverse solanaceous species. Plant Cell Rep. 2012;31:1713–22.
- Simmons CW, VanderGheynst JS, Upadhyaya SK. A model of Agrobacterium tumefaciens vacuum infiltration into harvested leaf tissue and subsequent in planta transgene transient expression. Biotechnol Bioeng. 2009;102(3):965–70.
- Chincinska IA. Leaf infiltration in plant science: old method, new possibilities. Plant Methods. 2021;17(1):1–21.
- Liu Y, Sun W, Zeng S, Huang W, Liu D, Hu W, Shen X, Wang Y. Virus-induced gene silencing in two novel functional plants, Lycium barbarum L. and Lycium Ruthenicum Murr. Sci Hortic. 2014;170:267–74.
- De Luca V, Salim V, Thamm A, Masada SA, Yu F. Making iridoids/secoiridoids and monoterpenoid indole alkaloids: progress on pathway elucidation. Curr Opin Plant Biol. 2014;19:35–42.

Liu et al. Plant Methods (2024) 20:26 Page 12 of 12

- Kulagina N, Meteignier LV, Papon N, O'Connor SE, Courdavault V. More than a Catharanthus plant: a multicellular and pluri-organelle alkaloid-producing factory. Curr Opin Plant Biol. 2022;67:102200.
- Qu Y, Safonova O, De Luca V. Completion of the canonical pathway for assembly of anticancer drugs vincristine/vinblastine in Catharanthus roseus. Plant J. 2019;97(2):257–66.
- 32. Caputi L, Franke J, Farrow SC, Chung K, Payne RME, Nguyen TD, Dang TT, Soares Teto Carqueijeiro I, Koudounas K, Duge, de Bernonville T et al. Missing enzymes in the biosynthesis of the anticancer drug vinblastine in Madagascar periwinkle. *Science* 2018, 360(6394):1235–1239.
- Singh SK, Patra B, Singleton JJ, Liu Y, Paul P, Sui X, Suttipanta N, Pattanaik S, Yuan L. Identification and characterization of transcription factors regulating Terpenoid Indole Alkaloid Biosynthesis in Catharanthus roseus. Catharanthus roseus: methods and protocols. Springer; 2022. pp. 203–21.
- Zhang H, Hedhili S, Montiel G, Zhang Y, Chatel G, Pré M, Gantet P, Memelink J. The basic helix-loop-helix transcription factor CrMYC2 controls the jasmonate-responsive expression of the ORCA genes that regulate alkaloid biosynthesis in Catharanthus roseus. Plant J. 2011;67(1):61–71.
- Sui X, Singh SK, Patra B, Schluttenhofer C, Guo W, Pattanaik S, Yuan L. Crossfamily transcription factor interaction between MYC2 and GBFs modulates terpenoid indole alkaloid biosynthesis. J Exp Bot. 2018;69(18):4267–81.
- Van Moerkercke A, Steensma P, Schweizer F, Pollier J, Gariboldi I, Payne R, Vanden Bossche R, Miettinen K, Espoz J, Purnama PC. The bHLH transcription factor BIS1 controls the iridoid branch of the monoterpenoid indole alkaloid pathway in Catharanthus roseus. Proc Natl Acad Sci USA. 2015;112(26):8130–5.
- Van Moerkercke A, Steensma P, Gariboldi I, Espoz J, Purnama PC, Schweizer F, Miettinen K, Vanden Bossche R, De Clercq R, Memelink J. The basic helixloop-helix transcription factor BIS 2 is essential for monoterpenoid indole alkaloid production in the medicinal plant Catharanthus roseus. Plant J. 2016;88(1):3–12.
- Singh SK, Patra B, Paul P, Liu Y, Pattanaik S, Yuan L. BHLH IRIDOID SYNTHESIS
   is a member of a bHLH gene cluster regulating terpenoid indole alkaloid biosynthesis in Catharanthus roseus. Plant Direct. 2021;5(1):e00305.
- Menke FL, Champion A, Kijne JW, Memelink J. A novel jasmonate-and elicitorresponsive element in the periwinkle secondary metabolite biosynthetic gene str interacts with a jasmonate-and elicitor-inducible AP2-domain transcription factor, ORCA2. EMBO J. 1999;18(16):4455–63.
- van der Fits L, Memelink J. ORCA3, a jasmonate-responsive transcriptional regulator of plant primary and secondary metabolism. Science. 2000;289(5477):295–7.
- 41. Paul P, Singh SK, Patra B, Sui X, Pattanaik S, Yuan L. A differentially regulated AP2/ERF transcription factor gene cluster acts downstream of a MAP kinase cascade to modulate terpenoid indole alkaloid biosynthesis in Catharanthus roseus. New Phytol. 2017;213(3):1107–23.
- 42. Singh SK, Patra B, Paul P, Liu Y, Pattanaik S, Yuan L. Revisiting the ORCA gene cluster that regulates terpenoid indole alkaloid biosynthesis in Catharanthus roseus. Plant Sci. 2020;293:110408.
- Paul P, Singh SK, Patra B, Liu X, Pattanaik S, Yuan L. Mutually regulated AP2/ ERF gene clusters modulate biosynthesis of Specialized metabolites in plants. Plant Physiol. 2020;182(2):840–56.

- 44. Sibéril Y, Benhamron S, Memelink J, Giglioli-Guivarc'h N, Thiersault M, Boisson B, Doireau P, Gantet P. Catharanthus roseus G-box binding factors 1 and 2 act as repressors of strictosidine synthase gene expression in cell cultures. Plant Mol Biol. 2001;45:477–88.
- Stavrinides A, Tatsis EC, Caputi L, Foureau E, Stevenson CE, Lawson DM, Courdavault V, O'Connor SE. Structural investigation of heteroyohimbine alkaloid synthesis reveals active site elements that control stereoselectivity. Nat Commun. 2016;7:12116.
- Wu Z, Singh SK, Lyu R, Pattanaik S, Wang Y, Li Y, Yuan L, Liu Y. Metabolic engineering to enhance the accumulation of bioactive flavonoids licochalcone A and echinatin in Glycyrrhiza inflata (licorice) hairy roots. Front Plant Sci. 2022:13:932594
- 47. Hiriart J-B, Lehto K, Tyystjärvi E, Junttila T, Aro E-M. Suppression of a key gene involved in chlorophyll biosynthesis by means of virus-inducing gene silencing. Plant Mol Biol. 2002;50:213–24.
- 48. Giuliano G, Bartley GE, Scolnik PA. Regulation of carotenoid biosynthesis during tomato development. Plant Cell. 1993;5(4):379–87.
- Qu Y, Easson ML, Froese J, Simionescu R, Hudlicky T, De Luca V. Completion of the seven-step pathway from tabersonine to the anticancer drug precursor vindoline and its assembly in yeast. Proc Natl Acad Sci U S A. 2015;112(19):6224–9.
- Vom Endt D, Soares e Silva M, Kijne JW, Pasquali G, Memelink J. Identification
  of a bipartite jasmonate-responsive promoter element in the Catharanthus
  roseus ORCA3 transcription factor gene that interacts specifically with ATHook DNA-binding proteins. Plant Physiol. 2007;144(3):1680–9.
- Mortensen S, Bernal-Franco D, Cole LF, Sathitloetsakun S, Cram EJ, Lee-Parsons CW. EASI transformation: an efficient transient expression method for analyzing gene function in Catharanthus roseus seedlings. Front Plant Sci. 2019;10:755.
- 52. Duge de Bernonville T, Clastre M, Besseau S, Oudin A, Burlat V, Glevarec G, Lanoue A, Papon N et al. Giglioli-Guivarc'h N, St-Pierre B: Phytochemical genomics of the Madagascar periwinkle: Unravelling the last twists of the alkaloid engine. *Phytochemistry* 2015, 113:9–23.
- Vázquez-Flotaand FA, De Luca V. Jasmonate modulates development-and light-regulated alkaloid biosynthesis in Catharanthus roseus. Phytochemistry. 1998:49(2):395–402.
- Soetaert SS, Van Neste CM, Vandewoestyne ML, Head SR, Goossens A, Van Nieuwerburgh FC, Deforce DL. Differential transcriptome analysis of glandular and filamentous trichomes in Artemisia annua. BMC Plant Biol. 2013;13(1):1–14.
- Wellburn AR. The spectral determination of chlorophylls a and b, as well as total carotenoids, using various solvents with spectrophotometers of different resolution. J Plant Physiol. 1994;144(3):307–13.

#### **Publisher's Note**

Springer Nature remains neutral with regard to jurisdictional claims in published maps and institutional affiliations.

# FISCAL YEAR 2025 – 2026 FINANCIAL REPORT



July 1, 2025 – September 30, 2025

QUARTERLY REPORT

TOBACCO RESEARCH INCOME										
	INCOME COMPARISON									
Fiscal Years	2019-2020	2020-2021	2021-2022	2022-2023	2023-2024	2024-2025	2025-2026			
July	\$141,864.01	\$136,565.92	\$102,816.87	\$113,853.04	\$-	\$97,579.97	\$84,421.42			
August	\$145,789.42	\$11,873.82	\$148,863.59	\$121,485.75	\$235,814.07	\$113,878.38	\$94,787.78			
September	\$132,169.60	\$261,157.23	\$138,395.19	\$143,503.64	\$116,834.55	\$112,212.24	\$109,954.48			
1st QUARTER	\$419,823.03	\$409,596.97	\$390,075.65	\$378,842.43	\$352,648.62	\$323,670.59	\$289,163.68			
October	\$150,849.00	\$141,682.93	\$138,913.78	\$131,512.77	\$84,290.07	\$86,565.34	\$-			
November	\$117,280.34	\$135,157.14	\$101,844.54	\$101,050.68	\$132,736.05	\$88,478.89	\$-			
December	\$151,323.23	\$159,616.92	\$138,232.14	\$113,515.64	\$81,648.61	\$90,136.26	\$-			
2nd QUARTER	\$419,452.57	\$436,456.99	\$378,990.46	\$346,079.09	\$298,674.73	\$265,180.49	\$-			
January	\$120,247.87	\$93,056.96	\$116,044.01	\$111,657.62	\$101,501.91	\$78,472.89	\$-			
February	\$114,095.14	\$125,797.09	\$89,271.71	\$78,955.86	\$77,922.09	\$125,701.11	\$-			
March	\$403,962.17	\$143,903.75	\$140,521.53	\$119,175.49	\$105,636.69	\$45,037.80	\$-			
3rd QUARTER	\$638,305.18	\$362,757.80	\$345,837.25	\$309,788.97	\$285,060.69	\$249,211.80	\$-			
April	\$117,862.64	\$144,970.47	\$127,449.97	\$79,639.90	\$119,161.48	\$94,449.22	\$-			
Мау	\$141,525.18	\$100,238.76	\$148,769.94	\$120,890.24	\$88,889.28	\$80,887.20	\$-			
June	\$138,849.18	\$211,130.06	\$121,204.33	\$149,991.92	\$154,407.96	\$103,211.51	\$-			
4th QUARTER	\$398,237.00	\$456,339.29	\$397,424.24	\$350,522.06	\$362,458.72	\$278,547.93	\$-			
TOTAL INCOME	\$1,875,817.78	\$1,665,151.05	\$1,512,327.60	\$1,385,232.55	\$1,298,842.76	\$1,116,610.81	\$289,163.68			

## **FISCAL YEAR 2025-2026**

# INCOME AND FINANCIAL REPORT

# KTRDC 1st QUARTER REPORT

					Prior Month	Current Month		YTD	
Funds Center	Funds Center Name	Category	Original Budget	Annual Budget	Balance	Actual	YTD Actual	Encumbrances	Available Budget
1235410080	KTRDC HOLDING ACCOUNT	Revenue	(\$1,723,000.00)			(\$109,954.48)	(\$289,163.68)		(\$1,433,836.32)
1235410080	Result	Total	(\$1,723,000.00)	(\$1,723,000.00)	(\$179,209.20)	(\$109,954.48)	(\$289,163.68)		(\$1,433,836.32)
1235410090	KENTUCKY TOBACCO RESEARCH BOARD	Operating Expenses		\$1,000.00					\$1,000.00
1235410090	Result	Total							
1235410090	Result	TOTAL		\$1,000.00					\$1,000.00
1235410100	KTRDC ADMINISTRATION	Salaries	\$1,723,000.00	\$260,000.00	\$28,779.46	\$14,564.24	\$43,343.70	\$138,752.29	\$77,904.01
1235410100	KTRDC ADMINISTRATION	Benefits			\$10,846.41	\$6,142.52	\$16,988.93	\$58,799.07	(\$75,788.00)
1235410100	KTRDC ADMINISTRATION	Operating Expenses			\$812.60	\$537.90	\$1,350.50	\$0.00	(\$1,350.50)
1235410100	KTRDC ADMINISTRATION	Recharges			\$6.81	\$5.97	\$12.78		(\$12.78)
1235410100	Result	Total	\$1,723,000.00	\$260,000.00	\$40,445.28	\$21,250.63	\$61,695.91	\$197,551.36	\$752.73
1235410110	KTRDC PERSONNEL	Salaries			\$69,101.97	¢20, 222 E7	\$101,435.54	¢202 201 40	(\$202,626,04)
	KTRDC PERSONNEL	Benefits				\$32,333.57			(\$303,636.94)
1235410110				<b>#4</b> 000 000 00	\$19,004.72	\$11,292.07	\$30,296.79		(\$91,759.92)
1235410110	KTRDC PERSONNEL	Operating Expenses		\$1,000,000.00	\$2,930.38	` '	\$1,054.85		\$998,945.15
1235410110	KTRDC PERSONNEL	Recharges		44 000 000 00	\$7,665.13		\$14,390.20		(\$14,390.20)
1235410110	Result	Total		\$1,000,000.00	\$98,702.20	\$48,475.18	\$147,177.38	\$263,664.53	\$589,158.09
1235410120	KTRDC PUBLICATIONS AND TRAVEL	Operating Expenses		\$25,000.00	\$21.20	\$3,810.81	\$3,832.01		\$21,167.99
1235410120	KTRDC PUBLICATIONS AND TRAVEL	Recharges			\$27.47	\$157.84	\$185.31		(\$185.31)
1235410120	Result	Total		\$25,000.00	\$48.67	\$3,968.65	\$4,017.32		\$20,982.68
1235410130	KTRDC BUILDING MAINTENANCE	Operating Expenses		\$50,000.00	\$11,123.48	\$748.34	\$11,871.82	\$0.00	\$38,128.18
1235410130	KTRDC BUILDING MAINTENANCE	Recharges		ψ30,000.00	\$1,473.12	\$129.33	\$1,602.45		(\$1,602.45)
1235410130	Result	Total		\$50,000.00	\$12,596.60	\$877.67	\$13,474.27	\$0.00	\$36,525.73
1233410130	nesuit	Totat		ψ30,000.00	Ψ12,530.00	ψ0/7.07	Ψ10,4/4.2/	ψ0.00	ψ30,323.73
1235410180	KTRDC SHOP	Operating Expenses		\$2,000.00	\$0.00		\$0.00		\$2,000.00
1235410180	Result	Total		\$2,000.00	\$0.00		\$0.00		\$2,000.00
1235410240	KTRDC LABORATORY EQUIPMENT	Operating Expenses		\$40,000.00	\$3,697.70	\$1,848.85	\$5,546.55		\$34,453.45
1235410240	Result	Total		\$40,000.00	\$3,697.70	\$1,848.85	\$5,546.55		\$34,453.45
					, , , , , , ,	, ,,	, , , , , , , , , , , , , , , , , , , ,		
1235410250	KTRDC UNALLOCATED RESERVE FOR RESEARCH	Operating Expenses		\$90,000.00					\$90,000.00
1235410250	Result	Total		\$90,000.00					\$90,000.00

## **FISCAL YEAR 2025-2026**

# INCOME AND FINANCIAL REPORT

# KTRDC 1st QUARTER REPORT

					Prior Month	Current Month		YTD	
Funds Center	Funds Center Name	Category	Original Budget	Annual Budget	Balance	Actual	YTD Actual	Encumbrances	Available Budget
1235410280	KTRDC GENERAL LABORATORY	Operating Expenses		\$50,000.00	\$4,375.12	\$1,088.65	\$5,463.77	\$0.00	\$44,536.23
1235410280	KTRDC GENERAL LABORATORY	Recharges			\$462.16	\$1.12	\$463.28		(\$463.28)
1235410280	Result	Total		\$50,000.00	\$4,837.28	\$1,089.77	\$5,927.05	\$0.00	\$44,072.95
1005 4110 40	VTDDC DICODETIONADV	Oneveting Evenence		#00 000 00	M144 FF	<b>#010.10</b>	#2FC CF		#10 C10 0F
1235411040	KTRDC DISCRETIONARY  KTRDC DISCRETIONARY	Operating Expenses		\$20,000.00	\$144.55	\$212.10 \$2.55	-		\$19,643.35
1235411040 1235411040	Result	Recharges		\$20,000.00	\$1.73 \$146.28	\$2.55	•		(\$4.28) \$19,639.07
1235411040	Result	Total		\$20,000.00	\$145.28	\$214.65	\$300.93		\$19,639.07
1235411310	KTRDC OUTREACH & COMMUNICATIONS	Operating Expenses		\$20,000.00					\$20,000.00
1235411310	Result	Total		\$20,000.00					\$20,000.00
1235411340	GENETIC MANIPULATION OF TOBACCO TO	Salaries							\$0.00
1235411340	GENETIC MANIPULATION OF TOBACCO TO	Benefits							\$0.00
1235411340	GENETIC MANIPULATION OF TOBACCO TO	Operating Expenses		\$30,000.00					\$30,000.00
1235411340	Result	Total		\$30,000.00					\$30,000.00
1233411340	nesuit	Totat		ψ30,000.00					ψ50,000.00
1235411360	PLANT BIOTECH METABOLIC	Operating Expenses		\$30,000.00	\$3,494.17	\$1,299.96	\$4,794.13	\$3,404.00	\$21,801.87
1235411360	PLANT BIOTECH METABOLIC	Recharges			\$40.70	\$11.87	\$52.57		(\$52.57)
1235411360	Result	Total		\$30,000.00	\$3,534.87	\$1,311.83	\$4,846.70	\$3,404.00	\$21,749.30
1235411370	KTRDC PLANT BIOTECH - MOLECULAR	Operating Expenses		\$30,000.00	\$3,374.17	\$7,150.59	\$10,524.76	\$127.40	\$19,347.84
1235411370	KTRDC PLANT BIOTECH - MOLECULAR	Recharges		<b>\$55,555.55</b>	\$2,349.59	\$490.41	\$2,840.00		(\$2,840.00)
1235411370	Result	Total		\$30,000.00	\$5,723.76	\$7,641.00			· · · · · · · · · · · · · · · · · · ·
1235411380	MOLECULAR GENETICS	Operating Expenses		\$30,000.00	\$1,995.21	\$81.94	. ,		\$27,922.85
1235411380	MOLECULAR GENETICS	Recharges			\$23.25	\$0.95	' '		(\$24.20)
1235411380	Result	Total		\$30,000.00	\$2,018.46	\$82.89	\$2,101.35	\$0.00	\$27,898.65
1235411410	KTRDC GREENHOUSE	Operating Expenses		\$15,000.00	\$83.15	\$83.45	\$166.60	\$1,768.60	\$13,064.80
1235411410	KTRDC GREENHOUSE	Recharges			\$742.38	\$611.50	\$1,353.88		(\$1,353.88)
1235411410	Result	Total		\$15,000.00	\$825.53	\$694.95			
4005444570	TORA COO MOLECULAR FARMINO A ORONOMICO	D. d. and a			ф0.00		φο οο		40.00
1235411570	TOBACCO MOLECULAR FARMING AGRONOMICS	Recharges			\$0.00		\$0.00		\$0.00
1235411570	Result	Total			\$0.00		\$0.00		\$0.00
1235412360	FLAVONOID - SMALLE	Salaries			\$1,776.50	\$934.99	\$2,711.49	\$3,416.04	(\$6,127.53)
1235412360	FLAVONOID - SMALLE	Benefits			\$898.80	\$454.00	\$1,352.80	\$1,493.66	(\$2,846.46)
1235412360	FLAVONOID - SMALLE	Operating Expenses		\$30,000.00					\$30,000.00
1235412360	Result	Total		\$30,000.00	\$2,675.30	\$1,388.99	\$4,064.29	\$4,909.70	\$21,026.01



Kentucky Tobacco Research & Development Center